Review article

Use of 3D-printed polylactic acid/bioceramic composite scaffolds for bone tissue engineering in preclinical in vivo studies: A systematic review

Iván Alonso-Fernández [a,*], Håvard Jostein Haugen [b], Mónica López-Peña [a], Antonio González-Cantalapiedra [a], Fernando Muñoz [a]

[a] *Anatomy, Animal Production and Veterinary Clinical Sciences Department, Veterinary Faculty, Universidade de Santiago de Compostela, Campus Universitario s/n, 27002 Lugo, Spain*
[b] *Department of Biomaterials, Institute of Clinical Dentistry, Faculty of Dentistry, University of Oslo, Oslo, Norway*

ARTICLE INFO

ABSTRACT

3D-printed composite scaffolds have emerged as an alternative to deal with existing limitations when facing bone reconstruction. The aim of the study was to systematically review the feasibility of using PLA/bioceramic composite scaffolds manufactured by 3D-printing technologies as bone grafting materials in preclinical in vivo studies. Electronic databases were searched using specific search terms, and thirteen manuscripts were selected after screening. The synthesis of the scaffolds was carried out using mainly extrusion-based techniques. Likewise, hydroxyapatite was the most used bioceramic for synthesizing composites with a PLA matrix. Among the selected studies, seven were conducted in rats and six in rabbits, but the high variability that exists regarding the experimental process made it difficult to compare them. Regarding the results, PLA/Bioceramic composite scaffolds have shown to be biocompatible and mechanically resistant. Preclinical studies elucidated the ability of the scaffolds to be used as bone grafts, allowing bone growing without adverse reactions. In conclusion, PLA/Bioceramics scaffolds have been demonstrated to be a promising alternative for treating bone defects. Nevertheless, more care should be taken when designing and performing in vivo trials, since the lack of standardization of the processes, which prevents the comparison of the results and reduces the quality of the information.

Statement of Significance

3D-printed polylactic acid/bioceramic composite scaffolds have emerged as an alternative to deal with existing limitations when facing bone reconstruction. Since preclinical in vivo studies with animal models represent a mandatory step for clinical translation, the present manuscript analyzed and discussed not only those aspects related to the selection of the bioceramic material, the synthesis of the implants and their characterization. But provides a new approach to understand how the design and perform of clinical trials, as well as the selection of the analysis methods, may affect the obtained results, by covering authors' knowledgebase from veterinary medicine to biomaterial science. Thus, this study aims to systematically review the feasibility of using polylactic acid/bioceramic scaffolds as grafting materials in preclinical trials.

1. Rationale

Bone defects are one of the most common tissue damages, originating from traumas, infections, tumor resection, reconstructive surgeries, congenital etiologies, etc. Resulting in significant detrimental effects on patient's quality of life and society [1–3]. Indeed, bone is the second most transplanted tissue after blood [4]. Al-

* Corresponding author at: Campus Universitario s/n, 27002 Lugo, Spain.
E-mail address: i.alonso.fernandez@usc.es (I. Alonso-Fernández).

though the vast majority of bone defects can heal spontaneously under suitable physiological and environmental conditions, bone healing is a complex physiological process that depends on the type and extent of the injury and patient's age and gender [3,5]. Large defects, also known as critical bone defects, may not heal spontaneously due to the size of the defect or unstable biomechanical properties, unfavorable wound environment, suboptimal surgical technique, metabolic factors, hormones, nutrition and applied stress [5]. The existing limitations facing bone reconstruction and repair have given rise to bone tissue engineering as an emerging and promising solution [6,7], and it has become one of the cornerstones of contemporary medical research since it was described in 1993. Significant innovation in this field to build functional structures to promote the regeneration of damaged or diseased organs has occurred in recent decades [7–9]

The ideal goal for regeneration is a newly developed bone tissue with the same immunological, functional, structural and mechanical characteristics as the native bone [10,11]. Thus, bone substitutes should be biocompatible, bioresorbable, osteoconductive and osteoinductive; finally replaced by newly formed bone. Furthermore, it should be easy to use, safe and cost-effective [1,12]. In order to meet these criteria, a large variety of biomaterials have been tested for in vivo bone tissue regeneration [1,8]. However, none of the currently available bone grafts possesses all the desirable characteristics such a biomaterial should have [4].

Biopolymers offer an alternative to traditional biocompatible materials (metallic and ceramic) and non-biodegradable polymers [13]. Specifically, polylactic acid (PLA) is a biocompatible, biodegradable, low cost and no toxic or carcinogenic polymer. Besides, it has an extensible mechanical property profile, ease of production, and high reproducibility thanks to additive manufacturing techniques [13–15]. Since PLA products were approved by the US Food and Drug Administration (FDA), in 1970, for direct contact with biological fluids, they have been used in relevant medical applications such as tissue engineering scaffolds, delivery system materials, covering membranes, different bio-absorbable medical implants and sutures [13,14]. However, PLA also presents several drawbacks, such as its slow degradation rate, hydrophobicity, and low cell affinity. Sometimes an inflammatory response from the contacting surrounding tissue can occur and its degradation products may increase the resorption site because of its acidity. Likewise, due to the importance of cell adhesion to the polymer, surface properties play a critical role, especially in biocompatibility, allowing vascular ingrowth, and cell attachment, migration, and proliferation. That is why different surface modification strategies have been developed to create desirable surface properties of PLA biomaterials, such as physical, chemical, plasma and radiation-induced methods, and the formation of coatings or composites [4,13,15].

A composite generally consists of two parts, the matrix and the reinforcing agent [15]. Among the wide range of materials that have been used for the synthesis of PLA composites, we are going to focus on bioceramics, which include calcium phosphates, the most widely used bone grafting materials due to their resemblance to the bone mineral phase, such as hydroxyapatite (HA) and β-tricalcium phosphate (β-TCP) [11,12]; and another promising group, the bioglasses (BG) or bioactive glasses, most of them based on the Na_2O, CaO, P_2O_5 and SiO_2 system, and with a weight percent of SiO_2 less than 55% [16–18]. They present sufficient biocompatibility, bioactivity, and bone conductivity, acting as a source of minerals for bone cells and not promoting an inflammatory response [7,16,17,19]. Furthermore, bioglasses can suppress growth of many, even multi-resistant, bacterial strains [16]. Despite that, they are brittle, have a low degradation rate, and lack mechanical characteristics (low fracture toughness) to form a high-quality scaffold by themselves [7,19]. However, bioceramics are suitable to be manufactured through additive manufacturing techniques, allowing the synthesis of 3D-printable composites when mixed with a polymeric matrix. Combining both materials can negate some of each other's disadvantages, improving their individual characteristics, such as better physical and mechanical properties, degradation rates and biosafety. And thus making them more attractive for their use in bone regeneration [15,19,20].

As well as FDA has approved PLA, bioceramic materials for its clinical use in humans, and different commercially available products can be found, such as Cerapatite® (HA), Cerasorb® (β-TCP) or BonAlive® (Bioglass) Since, the first formulation received the approval in 1996, a total of 15 HA, 21 β-TCP and 11 Bioglass products have been approved as of December 2020; even one PLA/HA composite, called SuperFIXSORB30® [21,22]. No human clinical trials using PLA/HA composites were found, however, Cannio et al. [18] did a literature review regarding the bioactive glass applications in human clinical trials, and Stachi et al. [23] compared synthetic hydroxyapatite with and inorganic bovine bone in sinus floor elevation in humans (ClinicalTrials.gov Identifier NCT03077867).

The advancement and creation of additive manufacturing techniques have provided researchers with a tool to create intricate replicable scaffolds for tissue regeneration. The demand for customizable bone substitutes has increased, and this technology has been shown to be able to create 3D porous scaffolds used for bone tissue engineering, because it allows the adaptation of the implants to the patient's specific bone geometry [7,13,24], based on the combined use of 3D image analysis, and computed tomography (CT) or magnetic resonance imaging (MRI) techniques [6,11]. Additive manufacturing is a promising 3D-printing method that allows the fabrication of customized 3D templates with complete control over the architecture, unlike conventional techniques such as gas foaming, sol-gel method, or freeze-drying [11]. Thus, it provides the necessary porosity and interconnectivity to access fluids and cells, favoring their migration, adhesion and proliferation, and effective transport of nutrients, oxygen, wastes, and growth factors. Hence, stimulating the continuous ingrowth of bone tissue form the periphery into the inner part of the scaffold (Fig. 1) [6,11].

Furthermore, before use in human beings as bone substitute, it should be tested both in vitro and in vivo to ensure it works effectively and safely, and for ethical, safety, economic and regulatory concerns [5,27]. 2D in vitro studies allow us to understand the mechanisms of bone repair at the cellular level and to assess biomaterials' biocompatibility. However, they oversimplify in vivo situations and do not give an overview of the whole tissue response [28]. Thus, pre-clinical models are necessary to simulate a clinical situation in a reproducible and easy-to-control manner, allowing us to evaluate a biomaterial's bioactivity, biocompatibility, toxicity, potential adverse reactions, or viability and efficacy [27,28]. They are based on similarities and analogies between humans and animals, and generally, the more similarities, the more suitable model [27].

Many reports have been published over the last years reviewing the possible use in bone tissue regeneration of different additive manufacturing technologies [6,7,11,15,29] and/or biomaterials, such as biopolymers [13,14], bioceramics [30] or composites [31,32]. However, most of them were focused on the manufacturing process, characterization aspects, or applications without paying much attention to their behavior when used in preclinical trials with animal models, which is a key factor of translational research. Tree systematic reviews addressed these issues. Hassan et al. [8] evaluate the effect of using 3D-printed templates on bone tissue regeneration in critical bone defects induced in experimental animal studies, specifically in calvaria defect models. Brunello et al. [12] investigated the result of applying bioceramic scaffolds, in terms of bone regeneration, for treating critical side defects in vivo. And finally Al-allaq and Kashan [33] reported a large-scale
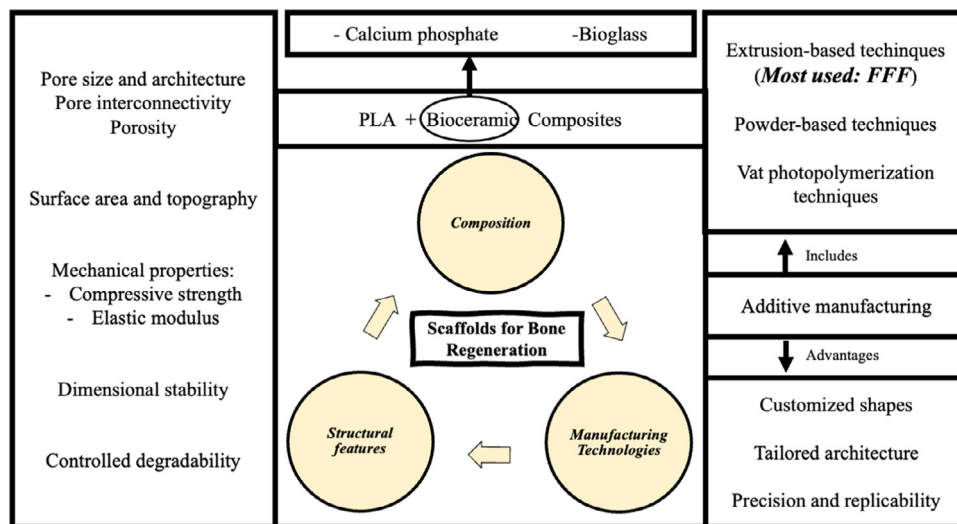
Fig. 1. Main features when synthesizing 3D-printed scaffolds for bone regeneration. PLA: polylactic acid; FFF: fused filament fabrication [4,7,10,11,25,26].

assessment of the capabilities of in vivo studies to generate an optimal regenerative process based on an analysis of the results after using bioceramics as bone substitute materials.

The purpose of the present study was to systematically review the feasibility of using PLA/bioceramic composite scaffolds manufactured by 3D-printing technologies as bone grafting materials in preclinical in vivo studies by evaluating their bone regeneration capabilities. However, this is not the only goal of the report, but also tries to carry out the importance of the different aspects to characterize when manufacturing 3D-printed scaffolds, and how they can affect to the bone healing process. Likewise, they authors highlight the importance of planning the clinical trials carefully, because of the implication that aspects such as the anesthetic protocol have on the result of the study.

2. Materials and methods

The present systematic review was conducted and reported according to the formal PRISMA guidelines ("Preferred Reporting Items for Systematic Reviews and Meta-Analyses"). However, ethics approval was not required for this review.

2.1. Search strategy

An electronic search was performed in the following health science databases: MEDLINE (PubMed) online library and Web of Science (WOS) database; it was carried out manually during February and September 2022. The search was limited to studies published in the last five years, considering the recent advancements in 3D-printing and biomaterial synthesis.

The studies were identified, based on different search strategies, using permutations of the following terms: "PLA", "Polylactic Acid", "PLLA", "poly (lactic) acid", "3D Print", "Three-dimensional print", "3D printing" "additive manufacturing" "material extrusion", "Scaffold", "Bone", "Bone regeneration", "Bone repair", "Bone reconstruction", "Bone tissue engineering", "In vivo", "Animal".

In addition, all the relevant articles found in the references and relevant review articles were checked and added as other sources.

2.2. Inclusion and exclusion criteria

2.2.1. Inclusion criteria
- Articles in English.
- Use of 3D-printed implants.
- In vivo animal model.
- Defined study parameters, including micro-tomographic (μCT) or histological evaluations of the bone formation.

2.2.2. Exclusion criteria
- Reviews and book chapters.
- In vitro studies or implants' characterization studies.
- Studies using PLA copolymers or non-bioceramic composites.
- Animal studies report ectopic bone formation models (e.g., subcutaneous).
- Studies using scaffolds loaded with chemotherapeutic agents, anti-inflammatory drugs and antibiotics.
- Use of PLA devices different from bone regeneration (e.g. screws or clips for fracture fixation).

Those studies including scaffolds with drugs/stem cells/substances affecting bone metabolism were not excluded.

2.3. Screening method and data extraction

A 2-stage screening was carried out. First, titles and abstracts were selected through an online search of inclusion. After removing duplicates, they were screened independently by two reviewers (I.A. and F.M.) using the inclusion and exclusion criteria. Next, the same two reviewers (I.A. and F.M.) carefully reviewed the full text of reports assessed for eligibility. For each study, relevant data were extracted and recorded on two previously designed data collection forms. One of them was dedicated to compiling the information referring to the biomaterials used, the manufacturing process of the scaffolds and their characterization; and the other one collected all the data related to the protocols for the in vivo preclinical test, grouping the animals according to the species, and the subsequent analysis of the obtained results. The final selection was based on the inclusion and exclusion criteria detailed above.

2.4. Quality assessment and risk of bias

Two independent authors (I.A. and F.M.) performed the quality and risk-of-bias assessments, and all authors resolved discrepancies with team consensus. To assess the quality of the included in vivo preclinical studies, we used the updated guidelines for reporting animal research: the ARRIVE guideline (Animals in Research: Reporting In Vivo Experiments) [34]. Specifically, we utilized the

"Compliance Questionnaire" to evaluate whether the reports complied with the ARRIVE Essential 10: Study design, sample size, inclusion and exclusion criteria, randomization, blinding, outcome measures, statistical methods, experimental animals, experimental procedures and results. Furthermore, we added the item "Adverse Events" because of its importance in a preclinical trial. Next, we categorized all the items as "reported", if the item was reported entirely, "not reported", if it was not reported, and "unclear" if it was partially reported or if insufficient details were provided.

The risk-of-bias in the manuscripts was assessed by using the SYRCLE (Systematic Review Centre for Laboratory animal Experimentation) tool [35] for animal studies in order to assign a judgment of low, high or unclear risk of bias to each of the 10 items included in the checklist evaluating 10 items: Allocation Sequence Generation, Baseline Characteristics, Allocation Concealment, Random Housing, Blinding of Care Giver/Investigator, Random Outcome Assessment, Blinding of Outcome Assessor, Incomplete Outcome Data Addressed, Free from Selective Outcome Reporting and Free from Other Sources of Bias. The methodological quality was analyzed by answering the main 10 questions as "yes", considered at low risk of bias, "no" which indicated a high risk of bias, or "unclear", for unclear items.

3. Results

3.1. Study selection

The literature search resulted in an initial pool of 799 potentially eligible publications collected from Pubmed and Web of Science. Once duplicates were removed, the remaining manuscripts ($n = 626$) were screened based on the tittle and the abstract, and after evaluating the inclusion and exclusion criteria, only 150 were included as potentially eligible for the present systematic review. After full-text analysis, 122 reports were excluded (Table 1), and 15 were not retrieved. Finally, the assessment of the references included from the initial pool led to a total of 13 articles that were found suitable to be included, in addition, an article was included by hand-searching. Thus, there are 14 publications to elaborate the present systematic review (Figure 2).

3.2. Study characteristics

Manuscripts included in this systematic review were mainly published after 2020 (8/13). Indeed 3D-printed scaffolds have become a promising alternative for bone regeneration. Hence, the interest in this production method has been growing for years.

The qualitative data of the studies have been extracted and displayed in the following analytic tables. From a total number of 14 included articles, 7 of them were conducted in rabbits, in which New Zealand rabbits were used [154–160], and another 7 ones in rats where used, two Wistar strain [161,162], four Spargue-Dawley [163–166] and in one the breed was not specificized [167]. According to the definition made by Brunello et al. [12], an intrabony defect of critical dimensional is not expected by definition, to heal

Table 1
Main Reason for exclusion after full-text screening.

Main Reason for Exclusion	No.	References
Language	2	[36,37]
Implants' characterization and/or in vitro study	48	[9,16,20,38–82]
No additive manufacturing fabrication	3	[83–85]
Ectopic bone formation model	2	[86,87]
PLA Copolymers	32	[19,88–118]
No PLA bioceramic composites	34	[119–152]
Internal Fixation Clip	1	[153]

spontaneously within the lifetime of the animal. All the defects made in rats were performed in calvaria, but only 3 could be considered as critical-sized bone defects (CSD). However, the ones in rabbits were performed in femur and radius, but only the ones in radius could be considered as CSD (Table 2). Zhang et al. [159], in contrast, did not make a defect, but rather developed a in vivo bioreactor model crossing the scaffold with a vascular bundle and transplanted it to tibial periosteum.

As mentioned before, PLA is one of the main polymeric materials used in bone tissue engineering, and its isomeric composition may vary its characteristics. Only four out of fourteen articles specify the isomeric, L- or D-LA, composition PLLA (pure poly L-LA, $n = 3$) [158,160,164] and PDLA (poly-D,L-LA, $n = 1$) [165]. Likewise, hydroxyapatite is the main bioceramic chosen for the synthesizing composites ($n = 10$) [154–161,163,166], being used as powders mixed in different ratios with the polymeric material. Besides, the HA particles' size varies among the publications, showing a nanometric size in 5 [154,156–158,163]. Other bioceramic materials employed are CaP ($n = 1$) [162] as a biomimetic coating, β-TCP ($n = 1$) [164], AW ($n = 1$) [165] or OCP ($n = 1$) [167].

Regarding the morphology of the scaffolds, the fabrication of 3D porous interconnected structures with different shapes and sizes has been the election in all the studies. These were probably selected for their advantages and crucial role in bone regeneration, simulating the properties of an extracellular matrix, to create a microenvironment conducive to optimal tissue regeneration. Among the wide range of production methods, additive manufacturing techniques can be divided in the following groups.

- Extrusion-based techniques, where the material is deposited using a nozzle fixed on a robotic arm, such as fused deposition modelling (FDM) or fused filament fabrication (FFF), robocasting, dispense plotting or bioplotting, multi-head deposition system (MHDS) or mini-deposition (MDS) system [7,11]. FDM or FFF is the most commonly used, as seen in 11 of the papers included in this review [154,156–163,165,166]. However, other alternatives when manufacturing 3D implants were utilized, such as micro-extrusion based 3D-printing technology ($n = 1$) [167] or 3D bioplotting ($n = 2$) [155,164].
- Other group is powder-based techniques, where particles constituting a powder are sintered or chemically bounded, such as inkjet printing, selective laser sintering (SLS), selective laser melting (SLM), binder jetting/sintering, direct metal laser sintering (DMLS) and electron beam melting (EBM) [7,11]. Binder jetting/sintering (indirect 3D-printing) technique was selected for the synthesis of apatite-wollastonite (AW) disks [165].
- Finally, vat photopolymerization techniques, where a liquid resin is photopolymerized using UV light.

Another important feature when synthesizing implants is the sterilization process since it is essential to prevent unsterile medical devices and also required to obtain regulatory approval [11,168]. Among the different sterilization techniques, ethylene oxide sterilization was selected to sterilize PLA-bioceramic composite scaffolds in 7 of the included manuscripts [154,159–163,166]; another paper utilized γ-irradiation [165] and in the remaining 6 studies the sterilization process was not reported [155–158,164,167]. Besides, Tcacencu et al. [165] used steam sterilization (also called autoclaving) to sterilize the apatite-wollastonite disks.

Scaffold characterization is an essential step in bone tissue engineering due to the importance of key parameters that may influence the biological response and the bone healing process, such as mechanical strength, porosity, degradability, or in vitro trials (summarized in Table 3). First, mechanical strength, in terms of compressive strength and/or elastic modulus, is included in approximately 57% of the studies, and its importance lies in its ability to withstand the existing loads after implantation and pro-

Identification of studies via databases and registers

Identification

Records identified from*:
- WOS (n=570)
- Pubmed (n=229)
(n = 799)

→

Records removed *before screening*:
Duplicate records removed
(n = 173)

Screening

Records screened
(n = 626)

→

Records excluded based on the title/abstract
(n = 476)

Reports sought for retrieval
(n = 150)

→

Reports not retrieved
(n = 15)

Reports assessed for eligibility
(n = 135)

→

Reports excluded after full-text screening (Table 1)
(n= 122)

Included

Studies included in review
(n = 13)
Reports included through manual searching
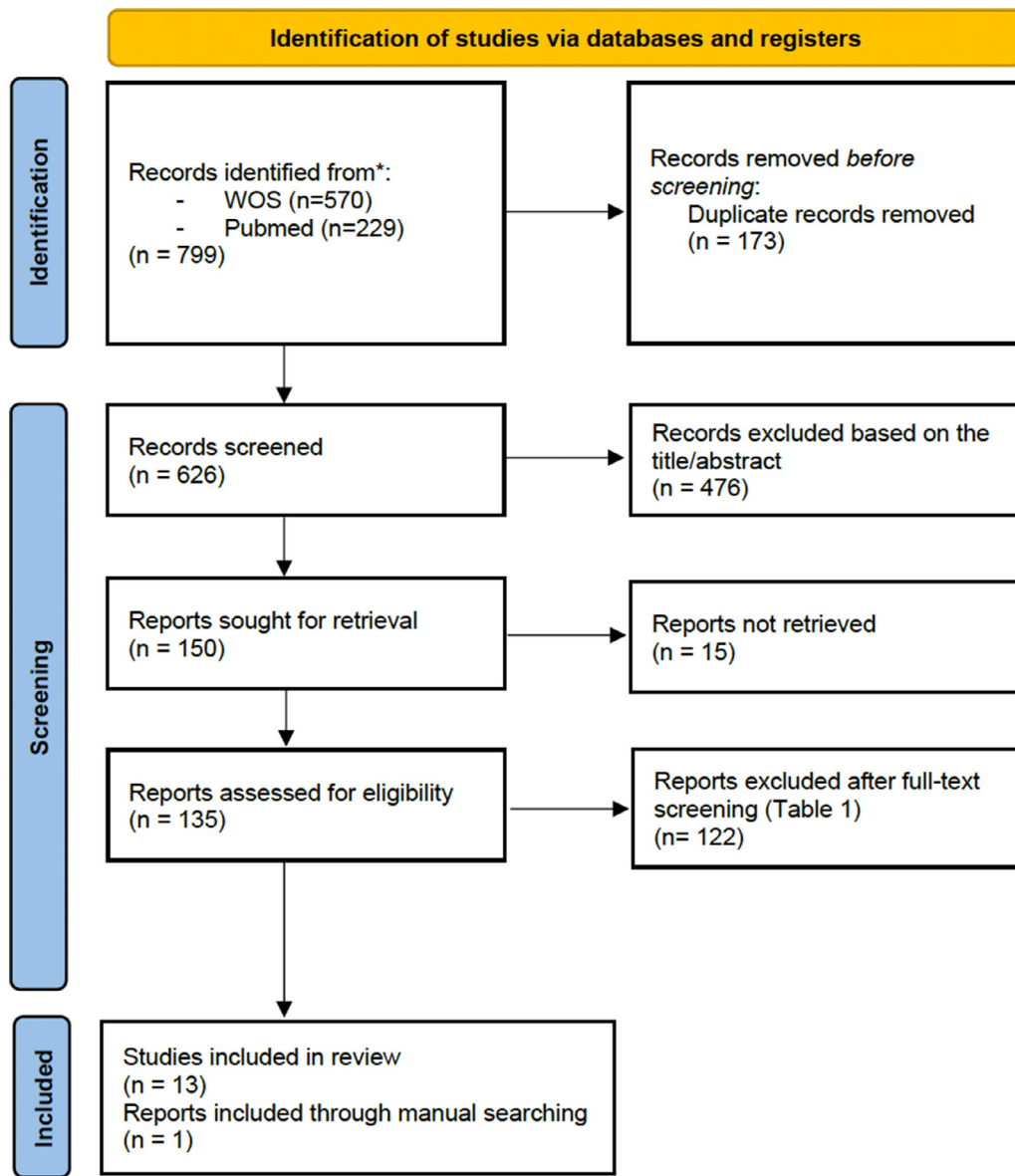(n = 1)

Fig. 2. Flow chart of the article selection procedure.

Table 2
Animal defects.

Animal	Study Model	Number of Publications	Critical-Sized Defects	References
Rats ($n = 7$)	Calvarial Bilateral Defect	1	1/1	[161]
	Calvarial Unilateral Defect	6	2/6	[162–167]
Rabbits ($n = 5$)	Femoral diaphysis defect (cylindrical)	4	0/4	[154,156–158]
	Radius diaphysis segmental defect	2	2/2	[155,160]

vide sufficient support to bone growth. So it should be as similar as possible to the bone: Compressive strength of Trabecular bone 0.1-16 MPa and Compressive strength of Cortical Bone 130-200 MPa [169,170]. Likewise, porosity and/or pore size have been reported in all the articles included in the present review as a consequence of its main role in cell spreading and effective transport of nutrients, oxygen, waste, etc., favoring continuous ingrowth of bone tissue from the periphery into the inner part of the scaffold [6,171,172]. Indeed, high porosity and pore size promote bone regeneration, but reduce the mechanical properties of the implant [172,173]. The results include values of porosity and pore size ranging between 26.4% and 70%, and 100 and 500 μm

respectively (See Table 3). However, the degradability of the scaffolds was only measured by 3 studies [156,158,164], even though it is an important parameter, as well as the degradation products derived from it, which can influence the environment affecting bone formation and healing time. Furthermore, the degradability will also be related to porosity and mechanical strength, as higher porosity leads to higher degradability and, consequently, a lower mechanical resistance [172,173]. In two of them, the samples were soaked into PBS media (pH 7.4 +- 0.2) at an established temperature, and variations in weight, molecular weight and/or pH were measured at various time points [156,158]. And in the other one, the analysis was performed in vivo, through the measurement

Table 3
Characterization of the scaffolds in the studies.

References	Biomaterials (s)	Mixing ratio (wt PLA: wt Bioceramic)	Bioceramic particle size	Production Method	Morphology	Porosity (%)	Pore Size (µm)	Elastic Modulus (GPa or MPa)	Compressive Strength (MPa)	In vitro	Degradability	Sterilization	Scaffolds analysis
[161]	PLA + HA	90: 10	50 µm	FFF	3D porous interconnected structure	58	450	-	-	-	-	Ethylene Oxide	SEM
[162]	PLA + CaP Coating	Uncoated / 98: 2	-	FDM	3D porous interconnected structure	49.93+-5.28 / 49.09±3.2	-	0.512±0.24 GPa / 0.510±0.11 GPa	20.50±1.95 MPa / 18.22±2.67 MPa	Yes	-	Ethylene Oxide	SEM, FTIR, XRD, TGA, Mechanical Test
[163]	PLA + n-HA	80:20	-	FDM	3D porous interconnected structure	70±2.23	-	10.12±1.24 GPa	31.18±4.86 MPa	Yes	-	Ethylene Oxide	SEM, Mechanical Test, Porosity evaluation
[164]	PLLA + β-TCP	100: 0 / 90: 10 / 70: 30	250 µm	3D Bioplotter	3D porous interconnected structure	~62	100		258±102MPa / 310±40MPa / 349±51MPa	Yes	PLLA/TCP30 % Remaining scaffold Week / GPC / NIR 4 / ~87 / ~91 8 / ~79 / ~84 12 / ~71 / ~69	-	SEM, µCT, Mechanical Test, Degradability test (GPC, NIR fluorescence imaging)
[165]	PLA + AW	70% AW, AW+30%MD powder (maltodextrin) 50:50	55% - 90 µm 15% - 0-53 µm	AW- Binder jetting/sintering (Indirect 3D-printing) PLA-FFF	3D porous interconnected structure	AW disks 41.85+-0.94% PLA 60%	-	-	-	Yes	-	AW – Autoclave PLA and composite – gamma radiation	SEM, µCT, Digital Microscope, XDR, Porosity evaluation (Archimedes method)
[166]	PLA + HA	85: 15	2.1±0.4 µm	MDS	3D porous interconnected structure.	60±1.5	500± 20	-	-	Yes	-	Ethylene oxide	SEM
[167]	PLA + OCP (octacalcium phosphate)	40: 60	-	MEB	3D porous interconnected structure.	-	500	-	1 MPa	Yes	-	-	FESEM, Mechanical Test
[156]	PLA + n-HA	100: 0 / 90: 10 / 80: 20 / 70: 30 / 60: 40 / 50: 50	50-80 nm	FDM	3D porous interconnected structure.	~50	-	-	~35MPa / ~29MPa / ~28MPa / ~25 MPa / ~23 MPa / ~17 MPa	Yes	Degradation rate: Pn50>Pn 30>Pn0	-	SEM, XDR, TEM, Mechanical Test; Porosity evaluation (Archimedes method), Degradability test (GPC)
[157]	PLA + n-HA	100:0 / 50: 50	75±20 nm	FDM	3D porous interconnected structure.	-	300-400	-	35.41±2.07 MPa / 17.8±1.92 MPa	Yes	-	-	TEM, AFM, SEM, EDS, µCT, Mechanical Test
[158]	PLLA + n-HA	100: 0 / 70: 30 / 50: 50	50-80 nm	FDM	3D porous interconnected structure.	60	-	43±0.09 MPa / 45.54±0.11 MPa / 44.31±0.10 MPa	44.02±6.85 MPa / 29.68±1.92 MPa / 14.22±0.20 MPa	Yes	Degradation rate and mass change: 50%n-HA>30%n-HA>0%n-HA	-	SEM, Contact angle, Mechanical test, Degradability test (GPC)
[155]	PLA + HA	70: 30	50 µm	3D Bioplotter	3D porous interconnected structure.	60	500	-	-	No	-	-	µCT, SEM
[154]	PLA + n-HA	90: 10	63±1.5nm	FDM	3D porous interconnected structure.	26.4	292±1.8	-	23.36±0.48 MPa	Yes	-	Ethylene oxide	SEM, EDS, Mechanical test, Porosity evaluation
[159]	PLA + HA	85: 15	2.1 ±1 µm	MDS	3D porous interconnected structure.	60	500	-	-	Yes	-	Ethylene oxide	-
[160]	PLA + HA	-	-	FDM	3D non-porous structure	-	-	-	-	No	-	Ethylene oxide	-

PLA: polylactic-acid); HA: hydroxyapatite; n-HA: nanohydroxyapatite; β-TCP: Beta-tricalcium phosphate; AW: apatite-wollastonite; OCP: octacalcium phosphate; wt: percentage by mass; FDM: Fused Deposition Modeling = FFF: Fused Filament Fabrication; MDS: Mini-Deposition System; MEB: Micro-extrusion based 3D-printing; SEM: scanning electron microscope; FTIR: Fourier transform infrared spectroscopy; XDR: X-ray diffraction; TGA: Thermogravimetric analysis; FESEM: field emission scanning electron microscope; TEM: Transmission Electron Microscope; AFM: Atomic Force Microscope; EDS: Energy-dispersive X-ray spectroscopy; µCT - Micro-computed tomography

of non-degradation-related molecular weights by gel permeation chromatography (GPC) and near-infrared (NIR) fluorescence images [164]. Finally, in vitro trials were carried out in all studies except three (see Table 3); though no information was collected, they represent an essential intermediate step between material synthesis and characterization, and in vivo testing. Scanning electron microscopy (SEM) is the most common characterization technique for scaffolds. However, others can be found in Table 3, such as Micro-Computed Tomography (μCT), mechanical testing, Fourier Infrared Spectroscopy (FTIR), Energy Dispersive Spectroscopy (EDS), X-ray Diffraction Analysis (XDR), etc.

Furthermore, different substances can be applied to scaffolds to improve bone healing and regeneration by affecting bone metabolism. Two studies used bone marrow-derived stem cells (BMSCs) [159,163], one used dental pulp stem cells (DPSC) [161] and one used enhanced bone marrow (eBM) [155]. Human osteoblastoma cell line (MG-63 cell line) was also used in one of the reports [164], as well as recombinant human bone morphogenetic protein-2 (rhBMP-2) [162]. Substances such as lanthanum (La), a rare earth element with an important role in the bone remodeling cycle that can promote the proliferation of bone-building osteoblast, were used in one paper [167]. Specifically in this case, La may influence the hydrolysis of OCP to an HA structure, thus influencing OCP mediated formation.

Likewise, many few procedures can also favor bone regeneration, such as sinusoidal electromagnetic fields (EMF) [163] or induced membrane technique (IMT) [155]. EMF triggered a higher new bone formation and vascularization. And IMT generated membranes similar to the periosteum, giving interesting results for treating large bone defects when combined with autografts [174].

There are different methods to assess bone healing in clinical trials. The ones utilized in selected studies are summarized in Tables 4 and 5. Histological evaluation was the most frequently used ($n = 14$), being able to distinguish between a qualitative histological analysis ($n = 13$), describing the results without the use of objective measurement techniques, and a quantitative or histomorphometric analysis ($n = 5$), that supplies objective data about the parameters analyzed such as angiogenesis or osteogenesis. In addition, these procedures can be carried out by decalcifying the bone and embedding it in paraffin ($n = 10$) or dehydrating and embedding it in a resin ($n = 4$). Likewise, micro-computed tomography analysis is widely used ($n = 9$), providing objective measurements to quantify bone regeneration. Other methods are radiographic evaluation, fluorescence imaging, immunohistochemistry (osteocalcin (OC), type I collagen (COL-1) or CD31) or biochemical analysis. Follow-ups varied between 4 and 16 weeks; a single observation time was reported in 4 out of 13 studies [158,160,161,165,167] and in the other ones, multiple observation times were chosen.

3.2.1. Studies in rats- main features

In vivo trials in the included reports for testing biomaterials were conducted through unilateral or bilateral defects in the calvaria of adult rats without any adverse reactions to the implanted scaffolds reported. The main characteristics and results of the studies are summarized in Table 4.

First, regarding the anesthetic protocols, different drugs and combinations were utilized by the different authors. Intraperitoneal injection of pentobarbital was administered in two studies, as a single drug [167], or in combination with inhaled isoflurane [163]. Ketamine was used alone [166], combined with xylazine [161,165], or with xylazine and midazolam [162]. Kwon et al. [164] chose a mixture of tiletamine, zolazepam and xylazine. Besides, only one study reports the use of local anesthesia, with lidocaine, and/or postoperative analgesia, in this case, buprenorphine [161]. Given the importance of the anesthetic protocol, both from

an ethical point of view and the experimental process, it will be analyzed in more in detail in the discussion section.

HA is the main bioceramic added to a PLA matrix for synthesizing composites, which will be later used to produce 3D porous scaffolds via 3D-printing. They were tested in rats in three selected studies [161,163,166]. Gendviliene et al. [161] manufactured PLA/HA scaffolds showed a low potential to induce bone growing (BV (mm3) μCT: male 3.86±0.99, new bone (mm2) histology: 2.90±0.06), that is slightly higher PLA alone scaffolds and negative control, but less than the one showed by the Bio-Oss (BV (mm3) μCT: male 4.24±0.51, new bone (mm2) histology: 4.15±0.58). However, these results can be improved by adding dental pulp stem cells to obtain a cellularized scaffold (PLA/HA cells), or the production of decellularized extracellular matrix PLA/HA (PLA/HA ECM) scaffolds from the first. Thus, achieving a bone formation in vivo similar o even superior to that obtained with the Bio-Oss (PLA/HA cells- BV (mm3) μCT: male 4.11±0.72, new bone (mm2) histology: 3.66±0.29; PLA/HA ECM- BV (mm3) μCT: male 5.09±1.27, new bone (mm2) histology: 3.80±0.24). Interestingly, significant differences between male and female groups can be appreciated in relation to bone growth (Figure 3).

Nevertheless, Zhang et al. [166] demonstrated the osteogenic capability of 3D-printed PLA/HA scaffolds, as confirmed by histological examination and the results of the tomographic analysis, which was performed at 4 and 8 weeks, showing that scaffolds' bone volume per total volume (BV/TV) presented values around 45% at 8 weeks. On the other hand, defects filled with β-TCP presented the highest BV/TV value, almost reaching 50%, and those filled with demineralized bone matrix (DBM) and the empty ones got the lowest values.

Tu et al. [163] utilized nano-grade HA to manufacture 3D-printed PLA/HA composite scaffolds. μCT results at 4 weeks after surgery indicate a BV/TV of about 10% approximately, a lower value than that obtained by Zhang et al. [166] at the same time point, approximately 20%. Histological and μCT results of the PLA/HA scaffold group are superior to the control group at both time points (PLA/HA BV/TV and New Bone Area Fraction (%) 4w and 8w: ∼10% and ∼20%). However, Tu et al. [163] applied two different treatments to PLA/HA scaffolds to improve their bone regeneration capability, seeding rat bone marrow mesenchymal stem cells (BMSCs), applying electromagnetic fields (EMF) or both, thus generating another 3 experimental groups. The results showed a higher percentage of bone growth in all groups, being more notable in the one that combined BMSCs and EMF (PLA/HA BMSCs + EMF BV/TV; 4w and 8w: ∼35% and ∼70%; New Bone Area Fraction (%) 4w and 8w: ∼30% and ∼60%). When used independently, the amount of new bone is lower without significant differences between PLA/HA BMSCs and PLA/HA EMF groups at any time point (Figure 4).

Almost no direct comparisons could be performed among papers that used HA in rat's calvaria model [161,163,166], because of differences in time points, PLA/HA mixing ratios and the defects' number and/or size.

Likewise, octacalcium phosphate (OCP) powders, which is thought to be one of the precursors for the formation of bone apatite crystals and can be converted to HA under physiological environments, were synthesized and mixed with PLA to create 3D-printed porous scaffolds [167]. OCP powders with different concentrations of Lanthanum (0.2/0.5/1La-OCP) were prepared via co-precipitation methods. In vivo trials showed that OCP promoted positive bone formation, an 0.2 La-OCP/PLA scaffolds showed an improvement in bone defect regeneration compared with the other groups.

β-tricalcium phosphate (β-TCP) was added to PLLA scaffolds by Kwon et al. [164], demonstrating effective support of bone regeneration. Micro-computed tomography showed a higher percentage of bone regeneration when a weight fraction (w.f.) of 30 TCP (∼25%

Table 4
Main features of studies in rats.

Reference	Animal	Anesthetic Protocol	Biomaterial groups	Sample Size	Defect	CSD	Empty Control	Groups	Bone metabolisms substances	Sacrifice Weeks	Assessment method	Main findings
[161]	Rat Wistar 300 gr 4 m/o 1/2 female y 1/2 male	Anesthesia: Ketamine 2.4 ml/kg, and Xylacine 5 mg/kg (IP) Local anesthesia: 2% Lidocaine 0.25 ml (SC) Postoperative Analgesia: Buprenorphine 0.01 mg/kg(SC)	PLA/HA	24	Calvarial Bone Circular bilateral defect ø 5.5 mm.	Yes	Yes	Empty $n = 8$ Bio-Oss $n = 8$ PLA $n = 8$ PLA/HA ($n = 8$) PLA/HA + DPSC ($n = 8$) PLA/HA + ECM ($n = 8$)	DPSC ECM	8 w	µCT analysis Qualitative histological analysis Quantitative histological analysis Paraffin	PLA/HA ECM scaffolds presented bone-forming ability comparable to that of Bio-Oss, based on histology and µCT analysis. Otherwise, PLA/HA scaffolds can potentially be used in bone tissue engineering, especially combined with the ECM.
[162]	Rat Wistar 300-400 gr	Anesthesia: Ketamine 100 mg/kg, Xylazine 10 mg/kg and Midazolam 5 mg/kg (IM)	PLA/CaP	45	Calvarial Bone Circular unilateral defect ø 8 mm	Yes	No	PLA $n = 15$ PLA/CaP $n = 15$ PLA/CaP + rhBMP2 $n = 15$	rhBMP-2	1, 3 and 6 m	Qualitative histological analysis Histomorphometric analysis Paraffin	The clinical trials have shown that the PLA-CaP scaffolds have proven to be biocompatible, promoting new bone formation after 6 months, even without rhBMP-2, based on histological results.
[163]	Rat Sprague-Dawley 280-320 g weight 12-13 w/0 male	Anesthesia: Pentobarbital 35 mg/kg and Inhaled Isofluorane	PLA/n-HA	126	Calvarial Bone Circular unilateral defect ø 6 mm	No	Yes	Empty=24 PLA/n-HA $n = 24$ PLA/n-HA + EMF $n = 24$ PLA/n-HA + BMSCs $n = 24$ PLA/n-HA + EMF + BMSCs $n = 24$	BMSCs Sinusoidal EMF: 15 Hz, 1mT. 4h/day)	4 and 12 w	µCT analysis Quantitative histological analysis Paraffin	The histological and microtomographic analysis revealed that PLA+HA scaffolds + BMSCs with EMF exposure present the best bone integration among all the groups, positioning itself as a promising candidate for craniofacial reconstruction.
[164]	Rat Sprague-Dawley 320-350 g. 8 w/o	Anesthesia: Combination of tiletamine and zolazepam, and Xylazine, 1:1, 1,5 mg/kg	PLLA/β-TCP	90	Calvarial Bone Circular unilateral defect ø 5 mm	No	No	PLLA $n = 15$ PLLA/TCP10 $n = 15$ PLLA/TCP30 $n = 15$ PLLA+MG63 $n = 15$ PLLA/TCP10 + MG63 $n = 15$ PLLA/TCP30 + MG63 $n = 15$	MG-63	4,8 and 12 w	µCT analysis Qualitative histological analysis Paraffin	3D-printed PLLA+TCP scaffold effectively supports bone regeneration in rats. The results show a greater bone regeneration rate in those animals with higher percent of TCP, and after adding of MG-63 to the scaffolds.
[165]	Rat Sprague-Dawley 350 g. adult male	Anesthesia: Ketamine and Xylacine	PLA/AW	15	Calvarial Bone Circular unilateral defect ø 8 mm	Yes	No	PLA dics $n = 3$ AW discs $n = 6$ AW/PLA discs $n = 6$	-	12 w	Qualitative histological analysis Histomorphometric analysis Paraffin	All three types of scaffolds were biocompatible. AW/PLA, the ones with the largest amount of new formed bone. AW scaffolds showed excellent osseointegration with the formation of new bone, and PLA ones have been well tolerated but were not osteogenic.
[166]	Rat Sprague-Dawley 300-350 g. 8 w/o Male	Anesthesia: Ketamine	PLA/HA	32	Calvarial Bone Circular unilateral defect ø 5 mm	No	Yes	3DP PLA/HA $n = 8$ β-TCP $n = 8$ DBM $n = 8$ Blank control $n = 8$	-	4 and 8 w	µCT analysis Qualitative histological analysis Immunohistochemistry (OC and COL-1) Paraffin	The percentage of new bone area in 3DP PLA/HA scaffolds was larger than in DBM (demineralized bone matrix) and control groups but less than β-TCP (Beta-Tricalcium phosphate) groups. The same tendencies were found at 4 and 8 weeks. So, PLA/HA scaffolds might be a promising candidate for bone defect repair, with little inflammation response, relatively larger resorption rate and superior osteoinductive activity.
[167]	Rat 6-8 w/o	Anesthesia: Pentobarbital (IP)	PLA/OCP	?	Calvarial Bone Circular unilateral defect. ø 5 mm	No	Yes	Control $n = ?$ PLA/OCP $n = ?$ PLA/OCP + 0.2La $n = ?$ PLA/OCP + 0.5La $n = ?$ PLA/OCP + 1La $n = ?$	La	8 w	Qualitative histological analysis Paraffin	The scaffolds enhanced bone defect regeneration in vivo. 0.2La-OCP/PLA scaffolds are significantly more likely to enhance bone defect regeneration in vivo than other groups. Our study suggests that La-OCP/PLA porous scaffolds have markedly potential in clinical bone tissue engineering.

m/o: months old; w/o: weeks old; PLA: polylactic-acid; HA: hydroxyapatite; n-HA: nanohydroxyapatite; β-TCP: Beta-tricalcium phosphate; AW: apatite-wollastonite; OCP: octacalcium phosphate; IP: intraperitoneal injection; SC: subcutaneous injection; IM: intramuscular injection; PLA:; HA:; n-HA:; OCP:; DPSC: dental pulp stem cells; ECM: extracellular matrix; rhBMP-2: recombinant human bone morphogenetic protein-2; BMSCs: bone marrow mesenchymal stem cells; EMF: electromagnetic fields; MG-63: human osteoblastoma cell line; DBM: demineralized bone marrow; La: Lanthanum; months: m; weeks: w; OC: osteocalcin; COL-1: type I collagen; µCT: micro-computed tomography.

Table 5
Main features of studies in rabbits.

Reference	Animal	Anesthetic Protocol	Biomaterial	Sample Size	Defect	CSD	Empty Control	Groups	Bone metabolisms substances	Sacrifice Weeks	Assessment method	Main findings
[156]	Rabbit New Zealand White 2-3 kg, male	Anesthesia: Pentobarbital 40 mg/kg (IV)	PLA/n-HA	18	Femoral Diaphysis Circular Unilateral Defect ø 5 mm	No	No	PLA n = 9 PLA/n-HA30% n = 9	-	4, 8 and 12 w	µCT analysis Qualitative histological analysis Resin	PLA/n-HA can be printed when the n-HA ratio is less than or equal 50%, the increasing incorporation of n-HA doesn't affect significantly the overall mechanical strength in a limited range (0-30%), but it really enhances the osteogenesis in vivo.
[157]	Rabbit New Zealand White 2-3 kg, male	Anesthesia: Pentobarbital 40 mg/kg	PLA/n-HA	-	Femoral Diaphysis Circular ¿Unilateral? Defect ø 5 mm	No	No	PLA n = ? PLA/n-HA 50% n = ?	-	1,2 and 3 m	µCT analysis Qualitative histological analysis Resin	The new bone growth of the composite material (PLA+50%n-HA) is significantly higher than that of the PLA group. Consequently, it has a high potential for use as implant for the critical bone defects
[158]	Rabbit New Zealand White 2-3 kg, male	Anesthesia: Pentobarbital 40 mg/kg (IV)	PLLA/n-HA	9	Femoral Diaphysis Circular bilateral Defect ø 5 mm	No	No	PLLA n = 3 PLLA/30%nHA n = 3 PLLA/50%nHA n = 3	-	4 w	Qualitative histological analysis Resin	The PLLA/50%n-HA has shown a preferable capability of bone regeneration, also supported by the discovery of the Harversian Canals, compared with the PLLA-30%n-HA specimens, which in turn have presented a bigger amount of new bone tissue than the PLLA ones.
[155]	Rabbit New Zealand White 2,5 +/- 0.25 kg, 6 m/o	Anesthesia: Pentobarbital 30 mg/kg (IM)	PLA/HA	36	Diaphysis Left Radius Segmental Unilateral Defect 15 mm	Yes	No	ICBG + IM n = 9 PLA/HA n = 9 IM + PLA/HA n = 9 IM + PLA/HA + eBM n = 9	eBM ICBG IMemb	4, 12 and 16 w	µCT analysis Qualitative histological analysis Histomorphometric Analysis Paraffin	The IM combined with 3D-printed PLA-HA scaffold and eBM has a bigger efficiency for treatment of large bone defects than the PLA-HA and the IM/PLA-HA groups, and similar to the IM/ICBG group (Gold Standard), based on the X-ray, µCT and histological results.
[154]	Rabbit New Zealand White 4.2+/-0.18 kg, male, adult	Anesthesia: Xylazine 0,1 ml/kg (IM)	PLA/n-HA	3	Distal Right Femur Circular Unilateral Defect ø 4.5 mm and Depth 10-13 mm	No	No	PLA/HA n = 3	-	4, 8 and 12 w	µCT analysis Qualitative histological analysis Resin	In vivo trials confirmed that the printed PLA/n-HA scaffold can enhance osteogenesis and osteoconductivity. It was showing bone formation within the femoral defect at 4,8 and 12 weeks, and no inflammation signs.
[159]	Rabbit New Zealand White 2.5+/-0.2 kg., 6 m/o	-	PLA/HA	24	Tibial Diaphysis Periosteum. Cuboid shaped periosteal pockets 10 mm in length and 7.5 mm in diameter.	-	No	Experimental Group (EG) PLA/HA +BMSCs with blood vessel Control Group (CG) PLA/HA + BM-SCs without blood vessel Control	BMSCs	4 and 8 w	µCT analysis Qualitative histological analysis Immunohistochemistry (OC and CD31) Paraffin	3D-printed PLA-HA composite scaffolds in an in vivo bioreactor prove to be a promising tool for the prefabrication of large volume, customized, vascularized bone tissues. Besides, adding a vascular bundle allows the construction of large vascularized bone grafts that translate into a bigger BV/TV, Tb.N and Tb.Th in the in vivo trials.
[160]	Rabbit 4-5.5 kg, female, > 7 m/o	Anesthesia: Ketamine 20 mg/kg, midazolam 2 mg/kg, and morphine 2 mg/kg (IM). Inhaled isoflurane Local anesthesia: 2% Lidocaine 6 mg/kg – Right brachial plexus block Postoperative Analgesia: Tramadol 4 mg/kg and meloxicam 0.1 mg/kg (SC)	PLA/HA	60	Diaphysis Right Radius Segmental Unilateral Defect 15 mm	Yes	Yes	Group n = 20 ICBG n = 20 PLA/HA Group n = 20	-	2, 4, 8 y 12 w	Radiographic analysis Qualitative histological analysis Paraffin	Scaffold created with anatomical characteristics similar to the radios proved to be biocompatible and allow cell multiplication around the composite. Despite of the fact that less bone callus and bone bridge was formed compared to the gold standard method (ICBG).

m/o: months old; w/o: weeks old; PLA: polylactic-acid; PLLA: poly-L-lactic-acid; HA: hydroxyapatite; n-HA: nanohydroxyapatite; IM: intramuscular injection; IV: intravenous injection; BMSCs: bone marrow mesenchymal stem cells; DBM: demineralized bone marrow; La: Lanthanum; eBM: enhanced bone marrow; ICBG: iliac crest bone graft; IMemb: induced membranes; w: weeks; m: months; OC: osteocalcin; µCT: micro-computed tomography; BV/TV: Bone Volume/Tissue Volume; Tb. N: Trabecular Number; Tb. Th: Trabecular thickness.
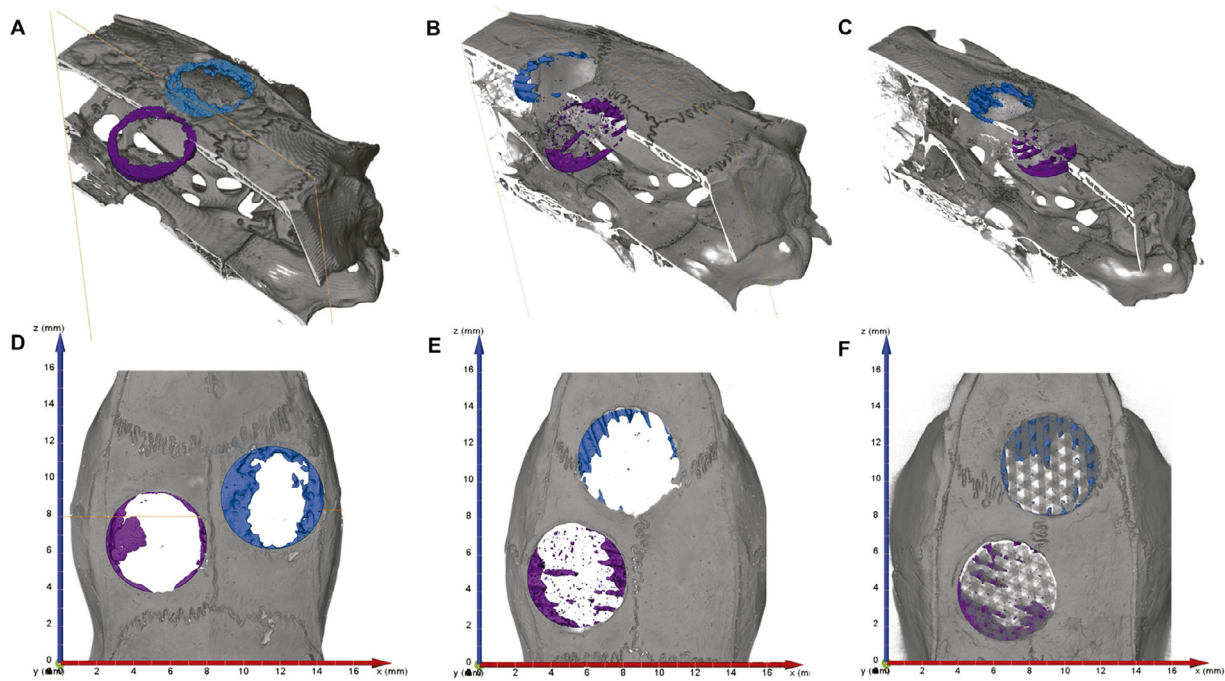
Fig. 3. μCT and histology results according to gender (All parameters are presented as mean SD). Processed μCT images taken with an X-Ray 3D Computer tomograph RayScan 250E. (a,d) Negative control (purple) and Geistlich Bio-Oss® (blue). (b,e) Pure PLA (blue) and PLA/HA (purple) scaffolds. (c,f) PLA/HA cellularized with dental pulp stem cells (blue) and PLA/HA Extra Cellular Matrix scaffolds (purple) [161]. "Reprint with permission from [161] under the terms of the Creative Commons Attribution 4.0 International License, CC BY-NC.ND 4.0."
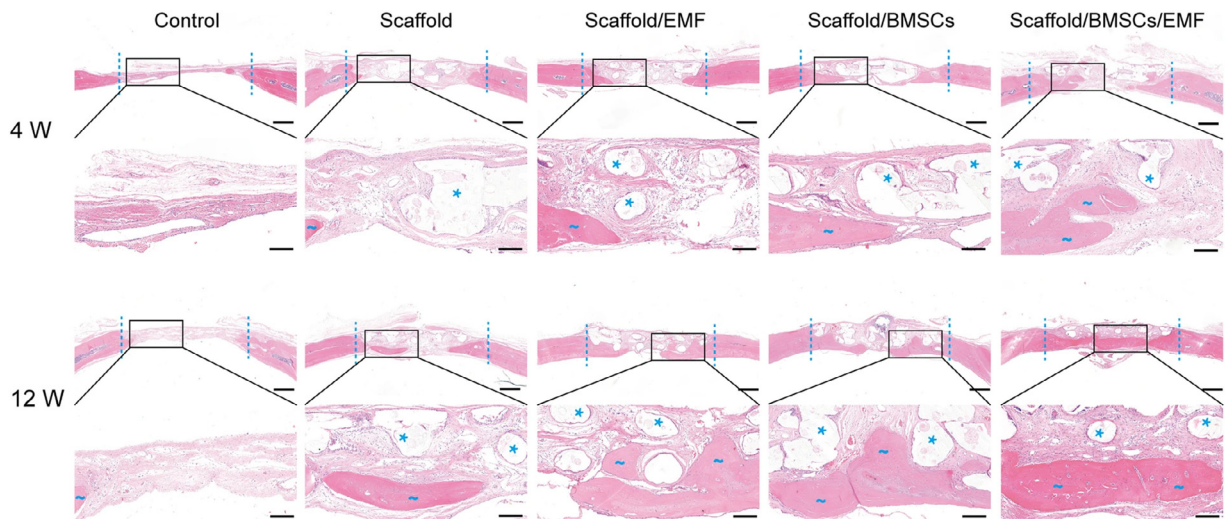
Fig. 4. Bone regeneration evaluated by HE staining. Coronal HE stained sections in the calvarial defect region of different groups were taken 4 and 12 weeks post-operation. The dotted line indicates the boundary of the 6-mm defect. Blue wary lines designate newly formed bone, and asterisks point to residual scaffolds. Scale bars in lower magnification images represent 1000 μm, and scale bars in higher magnification images represent 250 μm [163]. "Reprint with permission from [163] under the terms of the Creative Commons Attribution 4.0 International License, CC BY-NC.ND 4.0."

at 12 weeks) was used compared with PLLA/TCP10 w.f. (~10% at 12 weeks) or PLLA (~0% at 12 weeks) at all time points. The same trend was maintained when MG-63 cells were added to the scaffold, reaching 45% of bone regeneration values in the PLLA/30TCP group at 12 weeks. Besides, Massons's trichrome staining of cranial bone shows the formation of new bone tissue with a typical mature bone structure when MG-63 cells are added.

CaP biomimetic coatings have shown their capability to confer osteoconductivity properties to scaffolds. Maia-Pinto et al. [162] developed and evaluated PLA scaffolds biomimetically coated with apatite, with and without loading rhBMP-2. After 6 months, trim bone formation levels were appreciated in PLA group (New

formed bone: 11.2%), compared with PLA-CaP and PLA-CaP-BMP2 groups, which presented significantly better biological responses of newly formed bone, 31.2 and 44.85 respectively. Besides, PLA-CaP-BMP2 groups presented bone tissue formed with a more advance degree of maturity and large area, as compared to PLA-CaP group; and there was no significant degradation of the implants.

Finally, Tcacencu et al. [165] created a composite structure by manufacturing PLA and apatite-wollastonite (AW) disks combined with thermal bonding creating AW/PLA porous composite structures. Despite the confirmation by histological assessment of the in vivo biocompatibility of PLA, AW and AW/PLA scaffolds, the AW/PLA implants resulted in the most considerable amount of
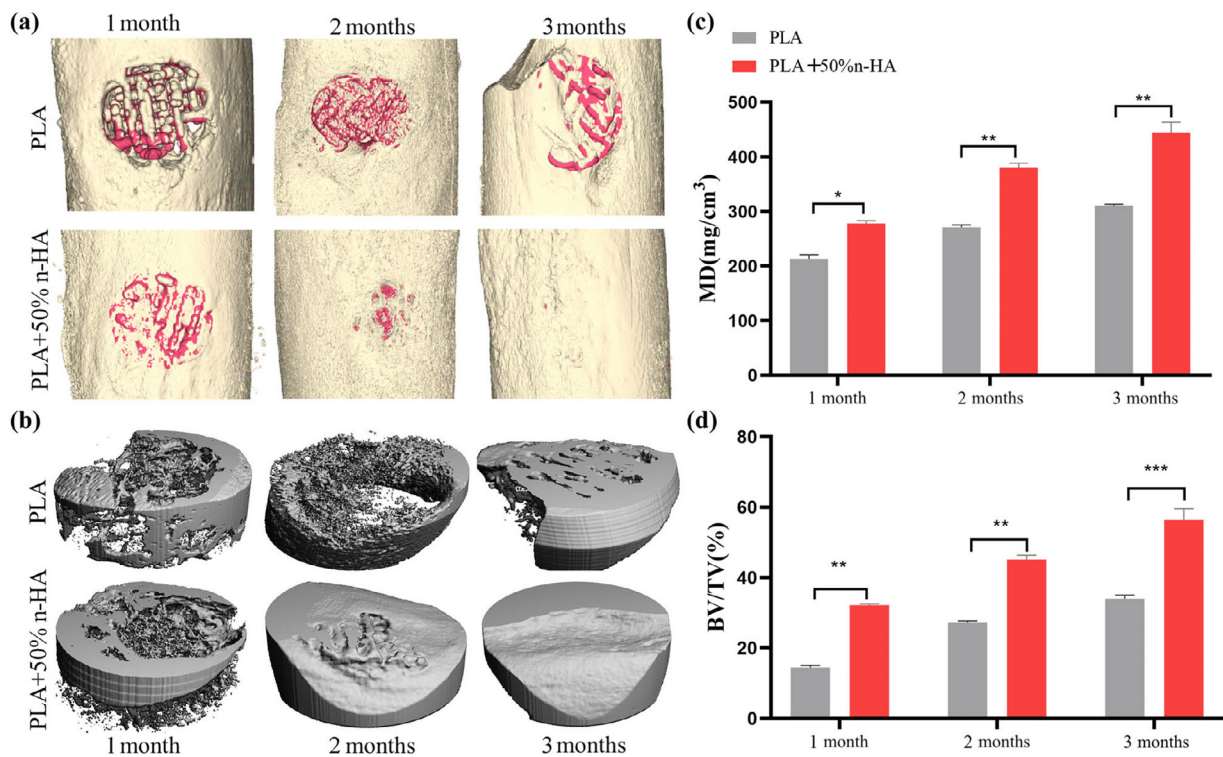
Fig. 5. Micro-CT analysis of the implanted scaffolds. The PLA and PLA/n-HA composite scaffolds were implanted into the rabbit femoral defect. (a) At 1,2 and 3 months after scaffold implantation, the bone defect area was scanned using micro-CT, and 3D reconstruction was performed. The reconstructed scaffold was shown in red and the bone in gold; (b) the scaffold-implanted area of the cortical bone (5 mm in diameter and 2 mm in depth) was reconstructed in 3D; and (c and d) quantitative calculation of new bone growth based on CT data, mineral density (MD), and bone tissue volume (BV)/total tissue volume (TV). $^{*}p < 0.05$; $^{**}p < 0.01$; $^{***}p < 0.001$. [157]. "Reprint with permission from [157] under the terms of the Creative Commons Attribution 4.0 International License, CC BY-NC.ND 4.0."

newly formed bone, with a percentage of newly formed bone between 15 and 25%, versus the 1-2% showed by AW implants.

3.2.2. Studies in rabbits

Studies in rabbits were performed on appendicular limbs, including the femur, tibia, and radius. No adverse effects were found when evaluating the behavior of the biomaterials. The main characteristics and results of the reports are summarized in Table 5.

Curiously, 4 out of the 7 anesthetic protocols selected in rabbits [155–158] included only an injection of pentobarbital, without the complementary administration of any drug. Regarding the other 3 studies, one reported using xylazine [154], and in the other one [159], no information about the anesthetic protocol was provided. Eventually, Minto et al. [160] selected combination of ketamine, midazolam and morphine for preanesthetic medication, besides they administered isoflurane for the induction and maintenance of the general anesthesia, and performed a right brachial plexus block using lidocaine. Likewise, authors used tramadol and meloxicam for postoperative pain control.

As it was mentioned above, HA is the most commonly used bioceramic, having been selected in all the studies in rabbits [154–160]. Specifically nano-HA, was utilized in 4 reports [154,156–158]; and 3 of them used a 5-millimeter circular defect in the femoral diaphysis to assess their bone regeneration properties [156–158]. Wang et al. [156] synthetized PLA/30%n-HA scaffolds and compared them with PLA/0%n-HA scaffolds. In vivo trials showed new bone tissue growing in all groups at any time points without inflammatory reaction or tissue necrosis, demonstrating the biocompatibility of the implant. µCT results indicate a higher bone growing in PLA/30%n-HA groups at 4, 8 and 12 weeks, with BV/TV percentages of 40% vs 30% in PLA/0%n-HA group. Wang et al. [157] manufactured 3D-printed porous scaffolds with a 5:5 mass

ratio PLA/n-HA showing that high n-HA content composite materials were biocompatible and osteogenic inductors conducting new bone growth at 1,2 and 3 months. Statistical differences ($p < 0.001$) were found when comparing BV/TV between PLA ($\sim$35% BV/TV at 3 months) and PLA/50%n-HA groups ($\sim$60% BV/TV at 3 months) (Figure 5). Likewise, these results were superior to those obtained by Wang et al. [156] at the same time point, 40% BV/TV PLA/30%n-HA vs 60% BV/TV PLA/50%n-HA, so a higher amount of n-HA on composites is related with a better bone regeneration of femoral defects. Zhang et al. [158], for their part, reported the implantation during 4 weeks of porous PLLA/n-HA scaffolds loaded with 0, 30 and 50% n-HA, and despite not having performed a quantitative analysis of the results, histological observations demonstrated that all the specimens utterly integrated with surrounding host tissue, with a little bone tissue formation in the internal pores of PLA/30% n-HA scaffolds and even less in PLLA ones, which presented the least new bone tissue. However, in the PLLA/50%n-HA scaffolds, all the pores were filled with new bone tissue, with signs indicating bone maturation. This reaffirms what was previously indicated about the relation between the presence of HA, and bone regeneration (Figure 6). The latest report on n-HA composites is the one carried out by Chen et al. [154], who developed porous PLA/n-HA composite scaffolds with the following PLA/n-HA mixing ratio 9:1 m/m, and evaluate its in vivo osteogenic effects by means of circular defects in the distal part of the femur. Quantitative analysis of µCT showed that BV/TV increased with the increased implant time, from 6% at 4 weeks to 20% at 12 weeks; besides the histological section indicated no inflammation signs and the presence of bone in bone/implant contact region and inside the pores.

No nano-hydroxyapatite powders were utilized in 3 reports in rabbits. Liu et al. [155] designed a 3D-printed scaffold with a PLA/HA mass ratio of 7:3, and tested it in long bone defects,
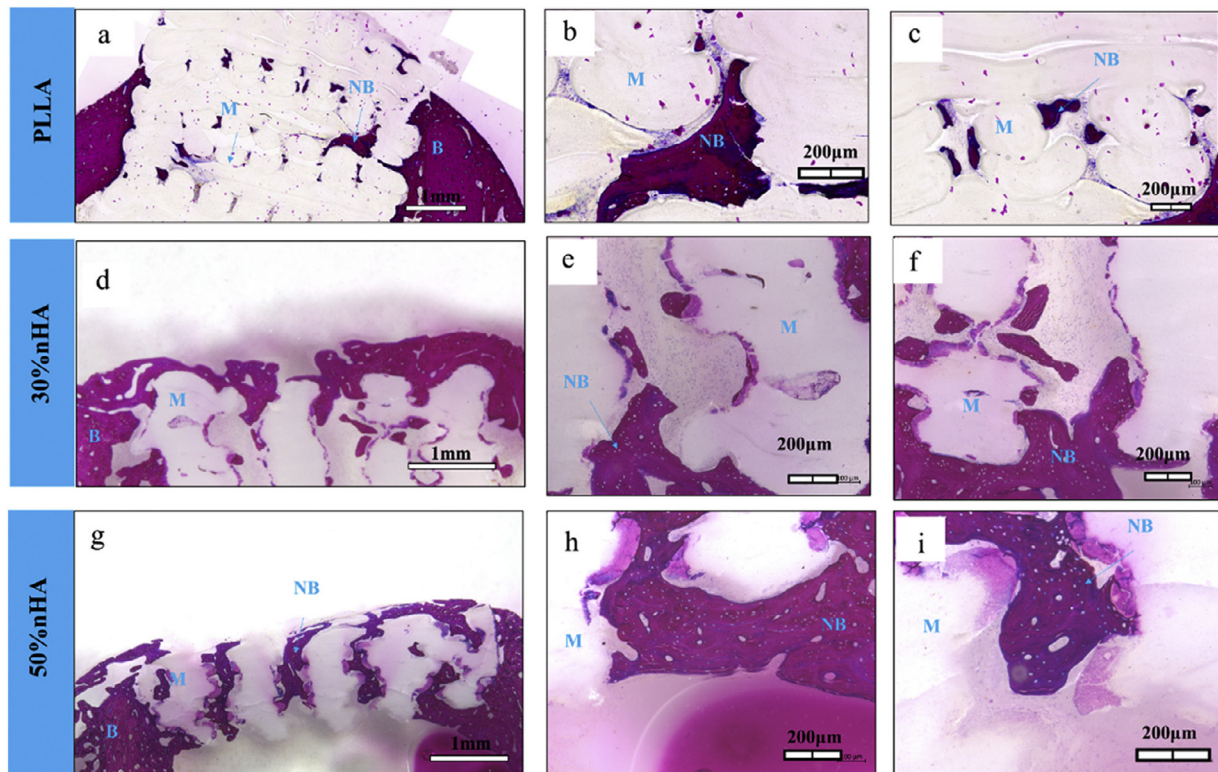
Fig. 6. HE evaluation of PLLA/nHA scaffolds in vivo for 4 weeks (a,d,g) cross-section HA histological images of PLLA, 30%nHA explants; (b,c) high magnification images of PLLA cross-sections and new bone; (e,f) high magnification images of 30%nHA cross-section and new bone; (h,i) high magnification images of 50%nH cross-sections and new bone (M: materials cross-sections, NB: new bone) [158]. "Reprint with permission from [158] under the terms of the Creative Commons Attribution 4.0 International License, CC BY-NC.ND 4.0."

specifically in a segmental defect in the middle of the left radius. Besides, they studied the effect of its use with induced membranes (IM), alone and combined with enhanced bone marrow (eBM), or iliac crest bone graft (ICBG), considered the gold standard in bone regeneration, to improve the bone healing process. Micro-tomographic analysis was performed at 16 weeks and showed the following results: PLA/HA group obtained the lowest BV/TV values (∼30%), then IM+PLA/HA group (∼50%), and finally IM+ICBG (∼70%) and IM+PLA/HA+eBM (∼70%), which had demonstrated the best effects on bone regeneration, without significative differences between them. Thus, IM and eBM significantly enhanced bone repair, achieving greater ratios of woven bone than PLA/HA and IM+PLA/HA groups. Likewise, histomorphometry results showed the same trend, with the following area ratios of WB at 8 weeks: PLA/HA (∼20%) < IM+PLA/HA (∼40%) < IM + ICBG (∼70%) = IM + PLA/HA + eBM (∼70%).

Minto et al. [160] manufactured a 3D-printed PLLA/HA non-porous scaffolds to fill a defect in the right radius diaphysis, and compared with empty control and iliac crest autologous graft groups. No severe lameness was detected in any of the groups, however, the implant groups showed grater lameness, edema, and pain, compared with the others. Likewise, radiographic and histopathologic studies showed smaller bone callous and grater inflammation signs, respectively, when animals included in PLLA/HA group were analyzed. Therefore, graft group was the one which led to superior results, since it is the gold standard for bone regeneration.

Finally, 3D-printed PLA-HA composites scaffolds were combined with in vivo bioreactor strategies to generate vascularized tissue-engineered bone of customizable size and geometry by Zangh et al. [159]. The scaffolds were seeded with autologous BMSCs, crossed with a vascular bundle (experimental group, EG) or not (control group, CG) and inserted in a tibial periosteum capsule. The histological examination revealed neovascular formation and ossified tissue regeneration in both groups at 4 and 8 weeks. Microangiography and μCT measurements showed a higher vessel number and volume in the EG than CG at any time point. In the same way, BV/TV analysis of the EG was significantly greater than CG, 35% vs 20% at 4 weeks, and 70% vs 30% at 8 weeks.

3.3. Study quality and risk of bias assessment

The quality assessment of the studies was performed according to the essential items of the ARRIVE guidelines, which are summarized in Figure 7. The individual analysis of the manuscripts showed that at item 3. "Inclusion and exclusion criteria", 6. "Outcome measures", 8. "Experimental Animals", 9. "Experimental Procedures", and 11. "Results" the information was adequate and reported with percentages of 85.7%, 78.6%, 85.7%, 64.3% and 64.3%; thus, it graded as "reported". However, items 4. "Randomisation", 5. "Blinding" and 10. "Adverse events" were considered as "not reported" because there is an evident lack of information in the reported studies, with frequencies 35.7%, 100% and 64.3%. Other items, such as 1. "Study Design", 2. "Sample Size" and 7. "Statistical Methods", were classified as "unclear reported", due to incomplete items reported, insufficient experimental details provided, or no subitems included.

The risk of bias was evaluated using the SYRCLE in all the included reports and is shown in the Figure 8, as a frequency distribution percent. Most of the questions were graded as "Low Risk of Bias", as shown in item 2. "Baseline characteristics", 6. "Random outcome assessment", 8. "Incomplete outcome data addressed", 9. "Free from selective outcome reporting" and 10. "Free from other sources of Bias", with percentages from 64.3% to 100%. By contrast,
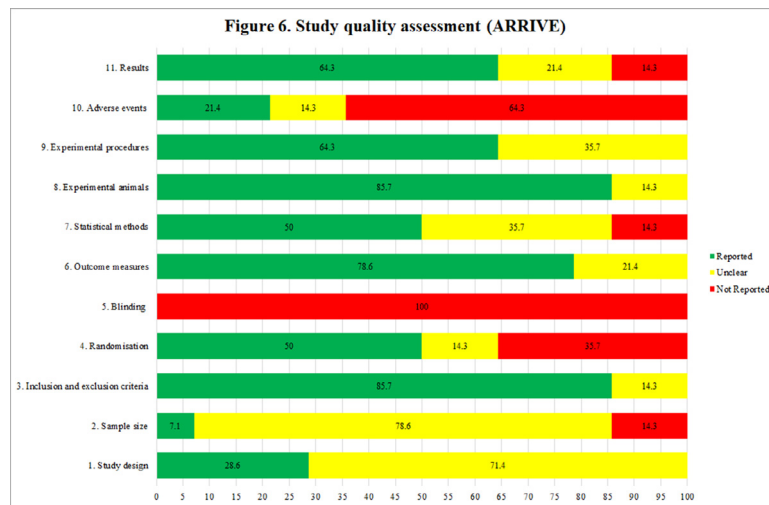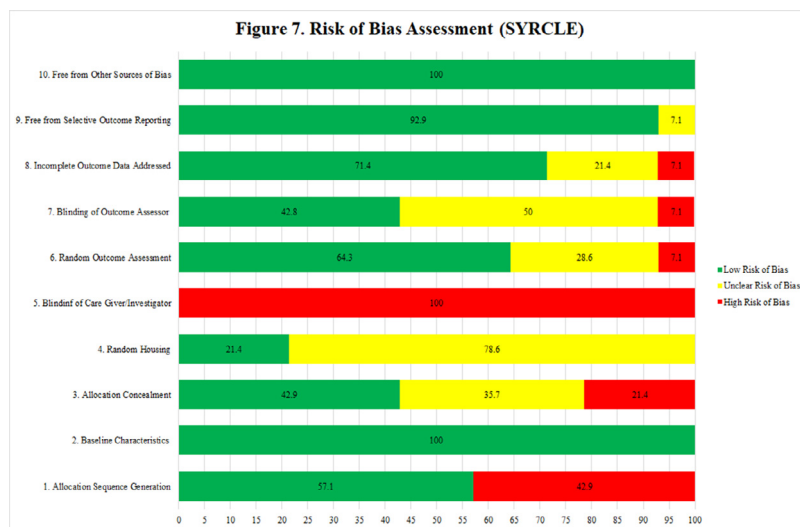
Fig. 7. Study quality assessment (ARRIVE).

Fig. 8. Risk of Bias Assessment (SYRCLE).

items 1. "Allocation sequence generation" and 5 "Blinding of care giver/investigator", were assigned as "High Risk of Bias" showing frequencies of 42.9% and 100%. Finally, "Unclear Risk of Bias" was detected at items 3 "Allocation concealment", 4 "Random housing" and 7 "Blinding of Outcome Assessor" with frequencies of 35.7%, 78.6% and 50%, respectively.

4. Discussion

This systematic review aimed to evaluate the possible use, as bone graft substitutes, of 3D-printed scaffolds synthesized from PLA/bioceramic composites in preclinical studies with animal models as a promising approach to bone repair and reconstruction. Bone tissue engineering is one of the main fields of study in biomedicine, due to the tremendous impact of this pathology on people's quality of life. Thus, the results positioned 3D-printing technology and composite materials as alternatives to heal impaired fractures, supporting and favoring the growth of new bone and vascular tissue. In addition, its implantation does not trigger and inflammatory response that could harm bone regeneration. Other authors have corroborated these findings, confirming that the use of 3D-printed templates showed more significant bone tissue regeneration than conventional porous templates fabricated from the same material [8]. Likewise, bioceramic scaffolds, alone or combined with polymeric materials, demonstrated better supported new bone formation, compared to untreated empty defects, and a similar bone growth compared to defects filled with deproteinized bovine-derived bone mineral [12].

The importance of using scaffolds in bone tissue engineering has increased in recent years, with the main goals of filling bone defects and supporting and inducing the growth of bone tissue [154]. At the same time, the utilization of additive manufacturing techniques for their synthesis has risen notably since it allows their customization when dealing with complicated and irregular geometries [175], as well as, precisely controlled architectures, high reproductivity and accuracy of produced parts [162,166]. In addition, scaffold architecture is critical for bone regeneration [161], because it is related to its ability to stimulate cellular responses and is essential for regulating cell adhesion, proliferation, migration, and differentiation.

Some of the scaffold's main studied parameters in the papers were the pore interconnection, overall porosity and pore size. A wide range of pore sizes can be selected for bone regeneration. Generally, macroporosity promotes osteogenesis and microporosity improves surface area for protein adsorption, providing attachment points for osteoblasts. Hence, studies suggested that pore

size should range from 200 to 500 micrometers. Typically, pores should be higher than 300 μm to facilitate osteoblast proliferation and enhance neovascularization, and 100 μm is the very minimum size, since it is associated with the formation of non-mineralised osteoid or fibrous tissue, limiting oxygen and nutrient diffusion throughout the scaffolds [4,161,171–173]. Likewise, pore interconnectivity positively influences bone deposition rate and depth of infiltration, improving nutrient and oxygen supply to the inner part of the scaffold and allowing cell infiltration [172,173]. Another feature that influences bone regeneration rate is the pore's geometry, due to different morphologies giving rise to differences in pore width and curvature of the surface, leading to variations in tissue morphology and growth rate. For example, tissue formation favors concave surfaces compared with flat and convex regions [172].

The bioactive properties are also important, and in all the studied publications, it was demonstrated that the addition of an appropriate amount of calcium phosphate to a PLA matrix provides the implant an improvement in its biological activity [156], by reducing possible inflammatory reactions that could limit PLA applications [166]. Likewise, the addition of bioceramics influenced mechanical properties and biodegradability. Balancing PLA's ductility and Ca-P's brittleness is the key issue regulating composite's mechanical properties [158]. Kwon et al. [164] observed that adding β-TCP in mixture ratios of 10 and 30%, increased the compressive strength of the implants from approximately 258 MPa (PLA alone), to 310 and 349 MPa respectively. However, other studies observed that when higher concentrations of hydroxyapatite were added to a PLA matrix, the compressive strength of the implants decreased [156–158]. Zhang et al. [158] showed that PLA scaffolds had a compressive strength of around 44.02 MPa, which decreased progressively as hydroxyapatite was added, with values of 29.68 and 14.22 MPa for 30 and 50%HA concentrations, respectively.

A critical property when manufacturing bone scaffold is its biodegradability. An ideal biodegradable material should be comparable to the rapid replacement rate by the new bone formation, providing support while leaving space for tissue growth [166]. Indeed, the degradation ratee should match the growth of native ECM to ensure mechanical support throughout the lifecycle of the scaffold [173]. PLA is degraded by simple hydrolysis, and the degradation products are then transformed into nontoxic subproducts that are eliminated through regular cellular activity and urine [13]. Nevertheless, lactate's releasing triggers the acidification of the environment affecting the defect site's acid-base balance, which can lead to hampered biological response towards the scaffold [24,156]. Like other bioceramics, HA performed the neutralizing capacity to the acidic products form in vivo degraded polymers and partially blocked the unfavorable acidic environment [154,176]. Besides, HA is hydrophilic, increasing the ability to absorb the water, and accelerating the degradation process [156,161]. Wang et al. [156] observed that Pn50 group (PLA/50%HA) degraded faster than the other groups (Pn30, PLA/30%HA and Pn0, PLA/0%HA) after 7 days. Zhang et al. [158] also obtained similar results with higher mass and molecular weight losses in PLA/50%HA scaffolds than PLA/30% HA and PLA/0%HA ones. Furthermore, the last studied changes in the solution pH values that before day 11 were significantly lower in PLA/50%HA and PLA/30%HA groups, corresponding to the degree of mass reduction. However, in the later stage, the high content of HA seemed to alleviate environmental acidity, and the lowest pH values were found in samples without HA. By contrast, Kwon et al. [164] concluded from their in vivo degradability analysis that 71% of the original molecular weight of the PLA scaffolds remains 12 weeks post-implantation, with similar results and consequently similar changes in the profiles, if the measures were obtained by GPC or NIR intensity. Besides, the degradation-related molecular weights of PLLA, PLLA+TCP10, and PLLA+TCP30 scaffolds did not vary significantly.

Regarding modifying the characteristics of PLA scaffolds, it is worth highlighting some of the available possibilities that may be interesting for bone tissue engineering. Shuai et al. [107] concluded in their work that the addition of poly (glycolic acid) (PGA) to PLLA/HA scaffolds results in an improvement of the hydrophilic behavior, with higher water absorption and the degradation rate, increasing the contact area between PLLA and body fluid. Consequently, there is a higher exposure of the HA embedded in the PLA matrix, which contacts with body fluids to exchange ions, and therefore the bone like apatite deposition, providing a suitable environment for osteoblastic growth and proliferation. Another possibility is using a copolymer of the PLA, derived from natural monomers of lactide and glycolide, such as poly (lactic-co-glycolic acid) (PLGA). Its amorphous structure allows water molecules to diffuse easily into the scaffold, providing greater degradability and bioactivity compared to the ones made by PLA [177].

Generally, when manufacturing the implants, the bioceramic powders were mixed or dissolved with PLA solution to be later printed using additive manufacturing techniques. However, Tcacencu et al. [165] synthesized apatite-wollastonite disks independently and then adhered them to PLA porous disks through a thermal bonding process, and Maia-Pinto et al. [162] biomimetically coated with apatite a 3D-printed polylactic acid scaffolds. Regarding the manufacturing process of PLA-HA implants, the most frequent combination, and the variations among the mixing ratios, it could be seen that most of the studies chose one proportion [154,155,157,159,161,163,166], but readers do not know why it was selected. However, others tested different concentrations of HA to evaluate the influence on scaffolds' performance [156,158]. At this point, it was observed that when HA ratio was more significant than 50%, the composite material could not be printed coherently and stably due to its high brittleness, but values less than or equal to 50% can be printed satisfactorily by FFF [156–158]. Zhang et al. [158] achieved a successful impression of a composite with 50% HA by using a silane couple agent called dodecyl trimethoxy silane (WD-10), which can combine with the polymer molecular chain more effectively. By contrast, Wang et al. [156] were able to print PLA/50%HA scaffolds but did not test them in vivo, probably because of the presence of apparent fractures in the cuboids and the negative effects of proportions of HA higher than 30% had over the ductility, as they reported.

HA particles' size is also another important aspect when synthesizing composites. Nano-hydroxyapatite has been demonstrated to overcome the shortcomings of the micro-sized one. It increases surface activity due to its size similar to apatite in natural bones, has better dispersibility to attach to the cell membrane and is more suitable as a filler or a coating material. Furthermore, it is less brittleness [156,157].

Likewise, sterilization processes have a major significance when manufacturing scaffolds for bone regeneration and need to be raised at the beginning of implant development. For this purpose, there are many available options as steam sterilization (also called autoclaving), ethylene oxide sterilization, hydrogen peroxide sterilization, γ-irradiation, electron-beam irradiation (also called β-irradiation) and UV sterilization. However, not all of them can be used on biodegradable polymers and/or bioceramics, because it may produce adverse reactions such as physico-chemical and morphological changes and the formation of toxic byproducts by degrading the material [11,168]. UV exposure, γ-irradiation and β-irradiation are suitable processes to sterilize biodegradable polymers. Nevertheless, autoclaving, plasma sterilization and ethylene oxide, the most used process in the included papers, should be avoided because they produce respectively, a shrinkage of the materials, physical alterations, and toxicity [11,178–180]. Regarding bioceramics, γ-irradiation has been shown to be the most indicate sterilization process. However, autoclaving and ethylene ox-

ide have been demonstrated to degrade some calcium phosphate phases [11,30]. Therefore, neither has proven suitable techniques for sterilizing composites synthesized from PLA and bioceramics.

Zeiter et al. [181] reported in their manuscript the massive variations in the chosen models used to test bone substitutes, for example, animal species, strain or breed, age and gender. Rabbits and rats were the most frequently used models but without a clear preference for a specific gender. Besides, there is a high variability in the age of the animals, something with critical influence regarding the closure of growth plates and the skeletal maturity. Literature revealed that important information such as age or gender, was missed in many studies, hindering the interpretation and replicability of the results. These results were in agreement with those obtained in the present review. Al-allaq and Kashan [33] also reported more trials in rodents (rats, mice), than in the rest of the models, probably because of the ease of handling and their small size. However, large animal models should be considered for future investigations, due to the similarities between human clinical conditions and animal models are essential for investigating bone scaffold interactions.

Among the species available for the evaluation of bone formation, rats and rabbits were selected for testing different composite materials in this review, and information about age or gender was variable between them or was not reported or specified [154–167]. Calvaria and femur were, respectively, the main anatomical regions selected to make the defects. However, because of protocol differences such as defect size, the number of defects, observation times or scaffolds composition, no cross-study comparisons could be performed, and the generalizability of the results was limited. Furthermore, the following limitations were found when evaluating the preclinical trials with animal models of the different reports. The sample size was not specified in two [157,167] and another one utilized only 3 animals [154], which is a deficient number of specimens to obtain significant statistical results. The critical-sized defect (CSD) model, commonly proposed for the evaluation of bone healing, was just observed in 5 papers [155,160–162,165]. The lack of control groups, since empty controls were only utilized in 5 of 14 studies [160,161,163,166,167], and iliac crest bone graft control or positive control in 2 [155,160]. The low report of adverse effects, usually present in this kind of procedure, was poorly reported, as seen in the study quality assessment. And finally, the absence of quantitative methods when evaluating bone regeneration among the different groups, such as μCT analysis, quantitative histologic analysis or histomorphometric analysis, was identified in 2 reports [158,160,167].

The choice of the anesthetic protocol is an essential step in the design of any animal experiment, and it must reach a state of unconsciousness, analgesia, and muscle relaxation. Scientists sometimes decide to leave the animals' pain untreated since using potent anesthetic and analgesic drugs may strongly affect the animals' biology. However, animal pain management in laboratories is an ethical imperative [182], specifically when performing most orthopedic and wound healing models, since they produce moderate to severe pain [183]. Below, we will analyze some of the main features of the drugs used for surgical procedures. Since pentobarbital is a barbiturate that produces hypnosis but has poorly analgesic properties, it is typically not used alone in painful procedures. It was administered alone in rabbits [155–158] and rats [167], although in the latter, it was combined in one case with isoflurane [163], an inhalational anesthetic with little or no analgesic activity. Ketamine is a dissociative anesthetic that reaches somatic analgesic levels. It was utilized in rats alone [166] or combined with other drugs, such as xylazine [161,165], xylazine and midazolam [162] or midazolam and morphine [160]. Xylazine is an alpha-2 agonist with powerful tranquillizing properties and moderate visceral analgesic action; midazolam, a benzodiazepine with relatively low

tranquillizing-sedative effects and no analgesic properties, is usually utilized as an adjunctive drug to ketamine; and morphine, a pure opioid with potent analgesic action and bad hypnotic properties, which is very useful given its lasting effects for animal's premedication, but also for the postoperative period. Tiletamine, as well as ketamine, is a dissociative anesthetic used in conjunction with zolazepam, a benzodiazepine drug; the combination provides a sedation, but no so potent analgesia. It was administered to rats in combination with xylazine [164]. Furthermore, only one two reports included the use of local anesthesia or postoperative analgesia. Gendviliene et al. [161] selected respectively, lidocaine, a short-acting local anesthetic commonly applied through the infiltration of the tissue, and buprenorphine, a partial agonist opioid which provides analgesia and is considered as an effective treatment for postsurgical pain. It is one of laboratory animals' most widely used analgesics [184]. Likewise, Minto et al. [160] administered lidocaine to perform a right brachial plexus block, a local anesthesia technique; and used meloxicam and tramadol for the control of the pain during the postsurgical period. Meloxicam is a non-steroidal anti-inflammatory drug (NSAID) which provides a moderate analgesic action, usually used for the treatment of pain or inflammatory processes. And tramadol is another opioid commonly administered in rabbits to treat mild acute and chronic pain, it has a low activity at the mu opioid receptor and inhibits noradrenaline and serotonin reuptake [185]. Doses and administration routes are highly important aspects when designing a protocol, although they will not be discussed in this paper. Once reviewed all the drugs included in the anesthetic protocol of the different studies, we can conclude that pain management is deficient in most of the articles, especially in the ones in rabbits. In addition, the use of local anesthesia techniques and postoperative pain control are non-standardized practices, at least in the papers included in the present review. But, what are the implications of choosing an ideal anesthetic protocol that includes an effective pain management, when designing an in vivo preclinical trial for the evaluation of biomaterials? Physiologic response to surgery and pain has been described as "surgical stress response". This phenomenon induced several changes in animals' physiology, such as muscle wasting, weight loss, impaired wound healing and a generalized state of immunosuppression, leading to the appearance of septic complications in the postoperative period. Furthermore, untreated pain can produce a reduction of food and water intake, disrupted sleep and changes in activity and behavior in rodents, which also can delay bone healing [183]. In matter of orthopedic procedures, pain control is also essential, because it favors continued limb usage, and thus, stimulate bone healing [183,186]. So, this is the reason why the concepts of balanced anesthesia and multimodal analgesia become important, since on the one hand they will help us to achieve a quick recovery and bone healing, and prevent chronic pain [183]. And on the other hand, it will allow us to reduce the possible bias outcomes that pain and stress can exert on the bone regeneration process in animals. The results of Carbone and Austin [182] also suggest that animal post-surgical pain is likely undertreated, likewise poor reporting of pain management can lead to the belief that analgesics are not or cannot be used, and as a consequence, other researchers published their work whit referring neither to pain or its treatment; so finally "under-reporting encourages under-treatment".

The urgent need to provide safe and effective biomaterials for clinical applications creates a demand for reproducible and technically simple bioassay for biomaterials' screening, which need to be tested at all stages of preclinical development [187,188]. Animal models play a key role in basic medical research, and many different ones have been used for different applications. [189,190]. However, they encounter ethical, practical, and technical problems which limit their use [190]. For this reason, other alternative pre-

clinical models have gained importance in recent years, thus promoting the incorporation of the 3Rs (Reduction, Replacement and Refinement) in submitted research proposals [188]. Cell cultures have been used as in vitro models for over a century and represents an indispensable tool to improve the understanding of cell biology and in vivo cell behavior mechanisms [189]. Different cell culture techniques have been developed. 2D monolayer models are simple and efficient to assess a biomaterial's biocompatibility, characterization and functionality. However they not accurately mimic the natural 3D organization of cells and their extracellular matrix [188,189], and consequently do not fully predict in vivo outcomes. This is why 3D cell cultures were developed, offering an opportunity to replace animal models due to their success to replicate a higher number of in vivo features by mimicking living organ's organization and microarchitecture (organotypic culture/organoids) [188,189]. Thus, 3D cell cultures allow the study of cell-cell and cell-environment interactions mimicking in vivo physiology [188]. Likewise, the chorioallantoic-membrane (CAM) of the chick embryo have demonstrated to be a valuable, short-term, simple and cost-effective assay to test biomaterials, with results comparable with the ones obtained in mouse trials [187,188,190]. The CAM functions as an organ for gas exchange between the embryo and the environment [187]. Its most common application is examining the angiogenic response as an early indicator of biomaterials' performance in vivo [188], because of the close connection between osteogenesis and angiogenesis during bone healing [190]. But this model also allows the evaluation of biocompatibility based on the survival rate of the chick embryos at the experimental end-point, the integration of the implant within the CAM and the presence of a primitive inflammatory response [188]. Finally, another option for the study of angiogenesis is the generation or an arteriovenous loop. This model is useful for investigating the angiogenesis and biocompatibility but also for the axial vascularization of scaffolds for tissue engineering purposes, in which engineered tissue can be transplanted with its vascular axis and connected to local vessels at the recipient site. The model provides the tissue with oxygen and nutrients immediately after transplantation [191].

3D-printed templates have been shown to have characteristics for their use in bone regeneration when composite originated from the addition of HA, β-TCP or octacalcium phosphate to a PLA matrix, the combination between PLA and apatite-wollastonite discs or the use of biomimetic CaP coatings; were utilized for their synthesis. Starting from this, we can extract certain ideas. First of all, we could see that higher concentrations of HA [156,158] or β-TCP [164], as expected, will lead to higher percentages of new bone area. Furthermore, the addition of different substances to functionalize the scaffolds, showed an improvement in the results compared with not functionalized groups, as Minto et al. [160] described in their paper "A factor that could assist the scaffold would be the use of precursor cells for osteogenesis to optimize bone healing, since biologically active 3D implants are promising in tissue regeneration". Dental pulp stem cells [161], bone marrow stem cells [159,163] or enhanced bone marrow [155], which increase the migration of the stem cells to the site of the injury, and induce angiogenesis and osteogenic differentiation by the release of growth factors. Indeed, grown factors with the greatest osteoinductive potential can also be applied, such as bone morphogenetic proteins (BMP) [162], which stimulate bone formation via recruiting osteoprogenitor cells. BMP-2 has been widely studied because of its ability to directly target BMP receptors at the cell surface and trigger stem cell differentiation in bone, and it has been demonstrated to be an alternative to stem cell implantation [192]. Likewise, other substances have demonstrated a positive effect on bone growth, such as human osteoblastoma cell lines [164], a potential osteoblast-like source. This potential osteoblast-like source allows rapid bone proliferation, and lanthanum, a foreign ion capable of

enhancing bone formation by influencing the hydrolysis of OCP to HA. Nevertheless, functionalizing substances is not the only strategy different authors use to stimulate bone regeneration. The application of electric fields [163] and induced membranes technique [155] have also benefited bone healing. Among the substances that can be added to scaffolds to improve the biological effects, even the use of metals has been reported. Wang et al. [193] recently published the addition of lithium to PLA/n-HA composites, which plays an important role in bone development, homeostasis, osteoblast differentiation and bone formation via the activation of Wnt signaling pathway. Likewise, in vivo trials have demonstrated that in lithium doped groups presented higher osteogenic induction than not doped ones.

As it could be seen in the results section, none of the papers matching the search criteria have used bioglass, however they have also been demonstrated to neutralize the acidic degradation of the PLA, improve the mechanical properties of the composites, as well as their bioactivity, cytocompatibility and biological fixation, defined as the capability of bonding to both hard and soft tissues. Furthermore, bioglass release inhibits the growth of various bacterial strains, reducing the risk of infections and implant encapsulation, as mentioned before [16,17]. Alksne et al. [20] in their work compared in vitro 3D-printed PLA/HA and PLA/BG composite scaffolds, and concluded that BG composites are more suitable for bone regeneration demonstrating better biofriendly and osteoinductive properties compared to pure PLA and PLA/HA scaffolds, since the ions dissociated from BG such as soluble silica, calcium, sodium and phosphate, stimulate osteogenesis and angiogenesis, affecting cell fate, biological response and osteogenic commitment more than HA, that only ensure bone building material accessibility acting as a nucleating site for bone minerals. Thus, BG is presented as another interesting option for the synthesis of composites for bone regeneration, as it was demonstrated by Sultan et al. [17] who implanted PLA/BG scaffolds subcutaneously in rats and reported the potential of these scaffolds in bone tissue engineering.

5. Conclusion

All included studies concluded that 3D-printed composite scaffolds provide a promising alternative for treating of bone defects. Tested implants showed to be biocompatible without the appearance of adverse reactions that could impair bone growth. They are also mechanically resistant, and bone formation was positively related to adding higher bioceramics to the PLA matrix. Furthermore, adding different substances to functionalize the scaffolds or using several procedures improved their biological activity and, consequently, the appearance of better newly bone formation results. However, most of the reports focused on the synthesis and characterization of the implant. Finally, they neglected the design and performance of in vivo trials with animal models, mainly in aspects related to anesthetic protocol, which is vital in this kind of study. Likewise, there is a lack of standardization in the design of these procedures that allows the comparison of the results obtained among the different reports, specifically when regarding the animal species, age and gender, the number and size of performed defects, the use of empty control groups, the establishment of critical defects as essential in the study of bone healing and the unification of formed bone quantification methods. These changes will lead to refining the surgical processes and procuring quality information without the risk of bias, which will help the rest of the research community working in this research area.

Declaration of Competing Interest

The authors declare that they have no competing of interests.

Acknowledgements

References

[1] G. Fernandez de Grado, L. Keller, Y. Idoux-Gillet, Q. Wagner, A.-M. Musset, N. Benkirane-Jessel, F. Bornert, D. Offner, Bone substitutes: a review of their characteristics, clinical use, and perspectives for large bone defects management, J. Tissue Eng. 9 (2018) 204173141877681, doi:10.1177/2041731418776819.

[2] A. Ho-Shui-Ling, J. Bolander, L.E. Rustom, A.W. Johnson, F.P. Luyten, C. Picart, Bone regeneration strategies: engineered scaffolds, bioactive molecules and stem cells current stage and future perspectives, Biomaterials 180 (2018) 143–162, doi:10.1016/j.biomaterials.2018.07.017.

[3] M. Majidinia, A. Sadeghpour, B. Yousefi, The roles of signaling pathways in bone repair and regeneration, J. Cell. Physiol. 233 (2018) 2937–2948, doi:10.1002/jcp.26042.

[4] H.J. Haugen, S.P. Lyngstadaas, F. Rossi, G. Perale, Bone grafts: which is the ideal biomaterial? J. Clin. Periodontol. 46 (2019) 92–102, doi:10.1111/jcpe.13058.

[5] Y. Li, S.K. Chen, L. Li, L. Qin, X.L. Wang, Y.X. Lai, Bone defect animal models for testing efficacy of bone substitute biomaterials, J. Orthop. Transl. 3 (2015) 95–104, doi:10.1016/j.jot.2015.05.002.

[6] G. Brunello, S. Sivolella, R. Meneghello, L. Ferroni, C. Gardin, A. Piattelli, B. Zavan, E. Bressan, Powder-based 3D printing for bone tissue engineering, Biotechnol. Adv. 34 (2016) 740–753, doi:10.1016/j.biotechadv.2016.03.009.

[7] A.V. Do, R. Smith, T.M. Acri, S.M. Geary, A.K. Salem, 3D Printing Technologies for 3D Scaffold Engineering, Elsevier Ltd, 2018, doi:10.1016/B978-0-08-100979-6.00009-4.

[8] M.N. Hassan, M.A. Yassin, S. Suliman, S.A. Lie, H. Gjengedal, K. Mustafa, The bone regeneration capacity of 3D-printed templates in calvarial defect models: a systematic review and meta-analysis, Acta Biomater. 91 (2019) 1–23, doi:10.1016/j.actbio.2019.04.017.

[9] A. Saberi, A. Behnamghader, B. Aghabarari, A. Yousefi, D. Majda, M.V.M. Huerta, M. Mozafari, 3D direct printing of composite bone scaffolds containing polylactic acid and spray dried mesoporous bioactive glass-ceramic microparticles, Int. J. Biol. Macromol. 207 (2022) 9–22, doi:10.1016/j.ijbiomac.2022.02.067.

[10] Tumedei, Savadori, Del Fabbro, Synthetic blocks for bone regeneration: a systematic review and meta-analysis, Int. J. Mol. Sci. 20 (2019) 4221, doi:10.3390/ijms20174221.

[11] C. Garot, G. Bettega, C. Picart, Additive manufacturing of material scaffolds for bone regeneration: toward application in the clinics, Adv. Funct. Mater. 31 (2021) 2006967, doi:10.1002/adfm.202006967.

[12] G. Brunello, S. Panda, L. Schiavon, S. Sivolella, L. Biasetto, M.D. Fabbro, The impact of bioceramic scaffolds on bone regeneration in preclinical in vivo studies: a systematic review, Materials 13 (2020) 1–26, doi:10.3390/ma13071500.

[13] M.S. Singhvi, S.S. Zinjarde, D.V. Gokhale, Polylactic acid: synthesis and biomedical applications, J. Appl. Microbiol. 127 (2019) 1612–1626, doi:10.1111/jam.14290.

[14] V. DeStefano, S. Khan, A. Tabada, Applications of PLA in modern medicine, Eng. Regen. 1 (2020) 76–87, doi:10.1016/j.engreg.2020.08.002.

[15] E.H. Tümer, H.Y. Erbil, Extrusion-based 3D printing applications of PLA composites: a review, Coatings 11 (2021) 390, doi:10.3390/coatings11040390.

[16] E. Schätzlein, C. Kicker, N. Söhling, U. Ritz, J. Neijhoft, D. Henrich, J. Frank, I. Marzi, A. Blaeser, 3D-Printed PLA-bioglass scaffolds with controllable calcium release and MSC adhesion for bone tissue engineering, Polymers 14 (2022) 2389, doi:10.3390/polym14122389.

[17] S. Sultan, N. Thomas, M. Varghese, Y. Dalvi, S. Joy, S. Hall, A.P. Mathew, The design of 3D-printed polylactic acid–bioglass composite scaffold: a potential implant material for bone tissue engineering, Molecules 27 (2022) 7214, doi:10.3390/molecules27217214.

[18] M. Cannio, D. Bellucci, J.A. Roether, Dino.N. Boccaccini, V. Cannillo, Bioactive glass applications: a literature review of human clinical trials, Materials 14 (2021) 5440, doi:10.3390/ma14185440.

[19] Y. Zhang, T. Lin, H. Meng, X. Wang, H. Peng, G. Liu, S. Wei, Q. Lu, Y. Wang, A. Wang, W. Xu, H. Shao, J. Peng, 3D gel-printed porous magnesium scaffold coated with dibasic calcium phosphate dihydrate for bone repair in vivo, J. Orthop. Transl. 33 (2022) 13–23, doi:10.1016/j.jot.2021.11.005.

[20] M. Alksne, M. Kalvaityte, E. Simoliunas, I. Rinkunaite, I. Gendviliene, J. Locs, V. Rutkunas, V. Bukelskiene, In vitro comparison of 3D printed polylactic acid/hydroxyapatite and polylactic acid/bioglass composite scaffolds: Insights into materials for bone regeneration, J. Mech. Behav. Biomed. Mater. 104 (2020) 103641, doi:10.1016/j.jmbbm.2020.103641.

[21] S. Dorozhkin, Medical application of calcium orthophosphate bioceramics, BIO 1 (2011) 1–51, doi:10.5618/bio.2011.v1.n1.1.

[22] S. Fukuba, M. Okada, K. Nohara, T. Iwata, Alloplastic bone substitutes for periodontal and bone regeneration in dentistry: current status and prospects, Materials 14 (2021) 1096, doi:10.3390/ma14051096.

[23] C. Stacchi, T. Lombardi, F. Oreglia, A. Alberghini Maltoni, T. Traini, Histologic and histomorphometric comparison between sintered nanohydroxyapatite and anorganic bovine xenograft in maxillary sinus grafting: a split-mouth randomized controlled clinical trial, BioMed Res. Int. 2017 (2017) 1–10, doi:10.1155/2017/9489825.

[24] J.-W. Kim, B.-E. Yang, S.-J. Hong, H.-G. Choi, S.-J. Byeon, H.-K. Lim, S.-M. Chung, J.-H. Lee, S.-H. Byun, Bone regeneration capability of 3D printed ceramic scaffolds, Int. J. Mol. Sci. 21 (2020) 4837, doi:10.3390/ijms21144837.

[25] S. Bose, S. Vahabzadeh, A. Bandyopadhyay, Bone tissue engineering using 3D printing, Mater. Today. 16 (2013) 496–504, doi:10.1016/j.mattod.2013.11.017.

[26] L. Roseti, V. Parisi, M. Petretta, C. Cavallo, G. Desando, I. Bartolotti, B. Grigolo, Scaffolds for bone tissue engineering: state of the art and new perspectives, Mater. Sci. Eng. C. 78 (2017) 1246–1262, doi:10.1016/j.msec.2017.05.017.

[27] A. Stavropoulos, A. Sculean, D.D. Bosshardt, D. Buser, B. Klinge, Pre-clinical *in vivo* models for the screening of bone biomaterials for oral/craniofacial indications: focus on small-animal models, Periodontol 68 (2015) 55–65, doi:10.1111/prd.12065.

[28] N. Donos, X. Dereka, N. Mardas, Experimental models for guided bone regeneration in healthy and medically compromised conditions, Periodontol 68 (2015) 99–121, doi:10.1111/prd.12077.

[29] A.T. Khalaf, Y. Wei, J. Wan, J. Zhu, Y. Peng, S.Y. Abdul Kadir, J. Zainol, Z. Oglah, L. Cheng, Z. Shi, Bone tissue engineering through 3D bioprinting of bioceramic scaffolds: a review and update, Life 12 (2022) 903, doi:10.3390/life12060903.

[30] N. Eliaz, N. Metoki, Calcium phosphate bioceramics: a review of their history, structure, properties, coating technologies and biomedical applications, Materials 10 (2017) 334, doi:10.3390/ma10040334.

[31] B.I. Oladapo, S.A. Zahedi, S.O. Ismail, D.B. Olawade, Recent advances in biopolymeric composite materials: future sustainability of bone-implant, Renew. Sustain. Energy Rev. 150 (2021) 111505, doi:10.1016/j.rser.2021.111505.

[32] R.A. Ilyas, S.M. Sapuan, M.M. Harussani, M.Y.A.Y. Hakimi, M.Z.M. Haziq, M.S.N. Atikah, M.R.M. Asyraf, M.R. Ishak, M.R. Razman, N.M. Nurazzi, M.N.F. Norrrahim, H. Abral, M. Asrofi, Polylactic acid (Pla) biocomposite: processing, additive manufacturing and advanced applications, Polymers 13 (2021), doi:10.3390/polym13081326.

[33] A.A. Al-allaq, J.S. Kashan, A review: in vivo studies of bioceramics as bone substitute materials, Nano Sel. 4 (2023) 123–144, doi:10.1002/nano.202200222.

[34] N. Percie du Sert, V. Hurst, A. Ahluwalia, S. Alam, M.T. Avey, M. Baker, W.J. Browne, A. Clark, I.C. Cuthill, U. Dirnagl, M. Emerson, P. Garner, S.T. Holgate, D.W. Howells, N.A. Karp, S.E. Lazic, K. Lidster, C.J. MacCallum, M. Macleod, E.J. Pearl, O.H. Petersen, F. Rawle, P. Reynolds, K. Rooney, E.S. Sena, S.D. Silberberg, T. Steckler, H. Würbel, The ARRIVE guidelines 2.0: updated guidelines for reporting animal research, PLOS Biol. 18 (2020) e3000410, doi:10.1371/journal.pbio.3000410.

[35] C.R. Hooijmans, M.M. Rovers, R.B. de Vries, M. Leenaars, M. Ritskes-Hoitinga, M.W. Langendam, SYRCLE's risk of bias tool for animal studies, BMC Med. Res. Methodol. 14 (2014) 43, doi:10.1186/1471-2288-14-43.

[36] F. Ze-wen, Z. Xin-yu, Q. Shuai, W. Yan, G. Jing, Q. Hui-xin, X. Lan-juan, 3D printing of polylactic acid/poly ethylene glycol/hydroxyapatite porous bone scaffolds and their biocompatibility, J. Mater. Eng. 49 (2021) 135–141, doi:10.11868/j.issn.1001-1381.2020.000390.

[37] S.M. Lebedev, D.M. Chistokhin, S. Shchadenko V, A.N. Dzuman, O.O. Nikolaeva, D. Mitrichenko V, A.B. Prosolov, I.A. Khlusov, Biodegradable polymer composites with osteogenic potential, Byulleten Sib. Meditsiny. 19 (2020) 119–129, doi:10.20538/1682-0363-2020-4-119-129.

[38] N. Ranjan, R. Singh, I.P.S. Ahuja, R. Kumar, D. Singh, S. Ramniwas, A.K. Verma, D. Mittal, 3D printed scaffolds for tissue engineering applications: mechanical, morphological, thermal, in-vitro and in-vivo investigations, CIRP J. Manuf. Sci. Technol. 32 (2021) 205–216, doi:10.1016/j.cirpj.2021.01.002.

[39] B. Ashwin, B. Abinaya, T.P. Prasith, S.V. Chandran, L.R. Yadav, M. Vairamani, S. Patil, N. Selvamurugan, 3D-poly (lactic acid) scaffolds coated with gelatin and mucic acid for bone tissue engineering, Int. J. Biol. Macromol. 162 (2020) 523–532, doi:10.1016/j.ijbiomac.2020.06.157.

[40] W. Clifton, E. Nottmeier, A. Damon, C. Dove, S.G. Chen, M. Pichelmann, A feasibility study for the production of three-dimensional-printed spine models using simultaneously extruded thermoplastic polymers, CUREUS 11 (2019), doi:10.7759/cureus.4440.

[41] M. Wan, S. Liu, D. Huang, Y. Qu, Y. Hu, Q. Su, W. Zheng, X. Dong, H. Zhang, Y. Wei, W. Zhou, Biocompatible heterogeneous bone incorporated with polymeric biocomposites for human bone repair by 3D printing technology, J. Appl. Polym. Sci. 138 (2021), doi:10.1002/app.50114.

[42] H. Belaid, S. Nagarajan, C. Barou, V. Huon, J. Bares, S. Balme, P. Miele, D. Cornu, V. Cavailles, C. Teyssier, M. Bechelany, Boron nitride based nanobiocomposites: design by 3D printing for bone tissue engineering, ACS Appl. Bio Mater. 3 (2020) 1865–1874, doi:10.1021/acsabm.9b00965.

[43] C.R. Moreno, E.M. Santschi, J. Janes, J. Liu, D. Kim, A.S. Litsky, Compression generated by cortical screws in an artificial bone model of an equine medial femoral condylar cyst, Vet. Surg. 51 (2022) 833–842, doi:10.1111/vsu.13814.

[44] H. Belaid, S. Nagarajan, C. Teyssier, C. Barou, J. Barés, S. Balme, H. Garay, V. Huon, D. Cornu, V. Cavaillès, M. Bechelany, Development of new biocompatible 3D printed graphene oxide-based scaffolds, Mater. Sci. Eng. C 110 (2020) 110595, doi:10.1016/j.msec.2019.110595.

[45] C.-H. Cheng, Y.-W. Chen, A. Kai-Xing Lee, C.-H. Yao, M.-Y. Shie, Development of mussel-inspired 3D-printed poly (lactic acid) scaffold grafted with bone morphogenetic protein-2 for stimulating osteogenesis, J. Mater. Sci. Mater. Med. 30 (2019), doi:10.1007/s10856-019-6279-x.

[46] M.-M. Liu, Y. Zhong, Y. Chen, L.-N. Wu, W. Chen, X.-H. Lin, Y. Lei, A.-L. Liu, Electrochemical monitoring the effect of drug intervention on PC12 cell damage model cultured on paper-PLA 3D printed device, Anal. Chim. ACTA. 1194 (2022), doi:10.1016/j.aca.2021.339409.

[47] Z. Huan, H.K. Chu, H. Liu, J. Yang, D. Sun, Engineered bone scaffolds with Dielectrophoresis-based patterning using 3D printing, Biomed. Microdevices. 19 (2017) 102, doi:10.1007/s10544-017-0245-5.

[48] R. Donate, M.Elena Aleman-Dominguez, M. Monzon, J. Yu, F. Rodriguez-Esparragon, C. Liu, Evaluation of aloe vera coated polylactic acid scaffolds for bone tissue engineering, Appl. Sci. 10 (2020), doi:10.3390/app10072576.

[49] K.S. Manjunath, K. Sridhar, V. Gopinath, K. Sankar, A. Sundaram, N. Gupta, A.S.S.J. Shiek, P.S. Shantanu, Facile manufacturing of fused-deposition modeled composite scaffolds for tissue engineering-an embedding model with plasticity for incorporation of additives, Biomed. Mater. Bristol. Engl. 16 (2020) 15028, doi:10.1088/1748-605X/abc1b0.

[50] A. Souness, F. Zamboni, G.M. Walker, M.N. Collins, Influence of scaffold design on 3D printed cell constructs, J. Biomed. Mater. Res. B 106 (2018) 533–545, doi:10.1002/jbm.b.33863.

[51] F. Caronna, N. Glimpel, G.-P. Paar, T. Gries, A. Blaeser, K. Do, E.B. Dolan, W. Ronan, Manufacturing, characterization, and degradation of a poly(lactic acid) warp-knitted spacer fabric scaffold as a candidate for tissue engineering applications, Biomater. Sci. 10 (2022) 3793–3807, doi:10.1039/D1BM02027G.

[52] M.P. Bernardo, B.C.R. da Silva, A.E.I. Hamouda, M.A.S. de Toledo, C. Schalla, S. Rütten, R. Goetzke, L.H.C. Mattoso, M. Zenke, A. Sechi, PLA/Hydroxyapatite scaffolds exhibit in vitro immunological inertness and promote robust osteogenic differentiation of human mesenchymal stem cells without osteogenic stimuli, Sci. Rep. 12 (2022) 2333, doi:10.1038/s41598-022-05207-w.

[53] P. Kowalczyk, P. Trzaskowska, I. \Lojszczyk, R. Podgórski, T. Ciach, Production of 3D printed polylactide scaffolds with surface grafted hydrogel coatings, Colloids Surf. B 179 (2019) 136–142, doi:10.1016/j.colsurfb.2019.03.069.

[54] R. Chung, D.M. Kalyon, X. Yu, A. Valdevit, Segmental bone replacement via patient-specific, three-dimensional printed bioresorbable graft substitutes and their use as templates for the culture of mesenchymal stem cells under mechanical stimulation at various frequencies, Biotechnol. Bioeng. 115 (2018) 2365–2376, doi:10.1002/bit.26780.

[55] M.J. Dewey, E.M. Johnson, D.W. Weisgerber, M.B. Wheeler, B.A.C. Harley, Shape-fitting collagen-PLA composite promotes osteogenic differentiation of porcine adipose stem cells, J. Mech. Behav. Biomed. Mater. 95 (2019) 21–33, doi:10.1016/j.jmbbm.2019.03.017.

[56] K. Dave, Z. Mahmud, V.G. Gomes, Superhydrophilic 3D-printed scaffolds using conjugated bioresorbable nanocomposites for enhanced bone regeneration, Chem. Eng. J. 445 (2022) 136639, doi:10.1016/j.cej.2022.136639.

[57] M. Alksne, E. Simoliunas, M. Kalvaityte, E. Skliutas, I. Rinkunaite, I. Gendviliene, D. Baltriukiene, V. Rutkunas, V. Bukelskiene, The effect of larger than cell diameter polylactic acid surface patterns on osteogenic differentiation of rat dental pulp stem cells, J. Biomed. Mater. Res. A. 107 (2019) 174–186, doi:10.1002/jbm.a.36547.

[58] S. Swetha, K. Balagangadharan, K. Lavanya, N. Selvamurugan, Three-dimensional-poly(lactic acid) scaffolds coated with gelatin/magnesium-doped nano-hydroxyapatite for bone tissue engineering, Biotechnol. J. 16 (2021) e2100282, doi:10.1002/biot.202100282.

[59] S. Pant, S. Thomas, S. Loganathan, R.B. Valapa, 3D bioprinted poly(lactic acid)/mesoporous bioactive glass based biomimetic scaffold with rapid apatite crystallization and in-vitro Cytocompatability for bone tissue engineering, Int. J. Biol. Macromol. 217 (2022) 979–997, doi:10.1016/j.ijbiomac.2022.07.202.

[60] B. Oladapo I, S.O. Ismail, M. Zahedi, A. Khan, H. Usman, 3D printing and morphological characterisation of polymeric composite scaffolds, Eng. Struct. 216 (2020), doi:10.1016/j.engstruct.2020.110752.

[61] F. Gang, W. Ye, C. Ma, W. Wang, Y. Xiao, C. Liu, X. Sun, 3D printing of PLLA/biomineral composite bone tissue engineering scaffolds, MATERIALS. 15 (2022), doi:10.3390/ma15124280.

[62] I. Buj-Corral, A. Bagheri, O. Petit-Rojo, 3D Printing of porous scaffolds with controlled porosity and pore size values, MATERIALS 11 (2018), doi:10.3390/ma11091532.

[63] L. He, X. Liu, C. Rudd, Additive-manufactured gyroid scaffolds of magnesium oxide, phosphate glass fiber and polylactic acid composite for bone tissue engineering, Polymers 13 (2021), doi:10.3390/polym13020270.

[64] C. Amnael Orozco-Diaz, R. Moorehead, G.C. Reilly, F. Gilchrist, C. Miller, Characterization of a composite polylactic acid-hydroxyapatite 3D-printing filament for bone-regeneration, Biomed. Phys. Eng. Express. 6 (2020), doi:10.1088/2057-1976/ab73f8.

[65] R. Donate, M. Monzon, Z. Ortega, L. Wang, V. Ribeiro, D. Pestana, J.M. Oliveira, R.L. Reis, Comparison between calcium carbonate and beta-tricalcium phosphate as additives of 3D printed scaffolds with polylactic acid matrix, J. Tissue Eng. Regen. Med. 14 (2020) 272–283, doi:10.1002/term.2990.

[66] E.H. Backes, L. de N. Pires, H.S. Selistre-de-Araujo, L.C. Costa, F.R. Passador, L.A. Pessan, Development and characterization of printablePLA/beta-TCPbioactive composites for bone tissue applications, J. Appl. Polym. Sci. 138 (2021), doi:10.1002/app.49759.

[67] M.P. Bernardo, B.C. Rodrigues da Silva, L.H. Capparelli Mattoso, Development of three-dimensional printing filaments based on poly(lactic

[68] V. Nadarajan, S.W. Phang, H.L. Choo, Fabrication of 3d-printed bone scaffold of natural hydroxyapatite from fish bones in polylactic acid composite, in: 13TH Int. Eng. Res. Conf. 13TH EURECA 2019, 2020, p. 2233, doi:10.1063/5.0001497.

[69] E.H. Backes, L.D.N. Pires, C.A.G. Beatrice, L.C. Costa, F.R. Passador, L.A. Pessan, Fabrication of biocompatible composites of poly(lactic acid)/hydroxyapatite envisioning medical applications, Polym. Eng. Sci. 60 (2020) 636–644, doi:10.1002/pen.25322.

[70] E. Salamanca, T.-C. Tsao, H.-W. Hseuh, Y.-F. Wu, C.-S. Choy, C.-K. Lin, Y.-H. Pan, N.-C. Teng, M.-C. Huang, S.-M. Lin, W.-J. Chang, Fabrication of poly-lactic acid/beta-tricalcium phosphate FDM 3D printing fiber to enhance osteoblastic-like cell performance, Front. Mater. 8 (2021), doi:10.3389/fmats.2021.683706.

[71] G. Dubinenko, A. Zinoviev, E. Bolbasov, A. Kozelskaya, E. Shesterikov, V. Novikov, S. Tverdokhlebov, Highly filled poly(l-lactic acid)/hydroxyapatite composite for3Dprinting of personalized bone tissue engineering scaffolds, J. Appl. Polym. Sci. 138 (2021), doi:10.1002/app.49662.

[72] S. Gnanamani Sankaravel, R.B. Syed, V. Manivachakan, In vitro and mechanical characterization of PLA/egg shell biocomposite scaffold manufactured using fused deposition modeling technology for tissue engineering applications, Polym. Compos. 43 (2022) 173–186, doi:10.1002/pc.26365.

[73] N. Soehling, M. Al Zoghool, E. Schaetzlein, J. Neijhoft, K.M.C. Oliveira, L. Leppik, U. Ritz, E. Doersam, J. Frank, I. Marzi, A. Blaeser, D. Henrich, In vitro evaluation of a 20% bioglass-containing 3D printable PLA composite for bone tissue engineering, Int. J. BIOPRINTING. 8 (2022) 65–81, doi:10.18063/ijb.v8i4.602.

[74] Y. Zamani, G. Amoabediny, J. Mohammadi, B. Zandieh-Doulabi, J. Klein-Nulend, M.N. Helder, Increased osteogenic potential of pre-osteoblasts on three-dimensional printed scaffolds compared to porous scaffolds for bone regeneration, Iran. Biomed. J. 25 (2021) 78–87, doi:10.29252/ibj.25.2.78.

[75] H. Hwangbo, J. Lee, G. Kim, Mechanically and biologically enhanced 3D-printed HA/PLLA/dECM biocomposites for bone tissue engineering, Int. J. Biol. Macromol. 218 (2022) 9–21, doi:10.1016/j.ijbiomac.2022.07.040.

[76] X. Lacambra-Andreu, N. Dergham, M. Magallanes-Perdomo, S. Meille, J. Chevalier, J.-M. Chenal, A. Maazouz, K. Lamnawar, Model composites based on poly(lactic acid) and bioactive glass fillers for bone regeneration, POLYMERS 13 (2021), doi:10.3390/polym13172991.

[77] A. Smieszek, K. Marycz, K. Szustakiewicz, B. Kryszak, S. Targonska, K. Zawisza, A. Watras, R.J. Wiglusz, New approach to modification of poly (l-lactic acid) with nano-hydroxyapatite improving functionality of human adipose-derived stromal cells (hASCs) through increased viability and enhanced mitochondrial activity, Mater. Sci. Eng. C 98 (2019) 213–226, doi:10.1016/j.msec.2018.12.099.

[78] C.-A. Dascalu, F. Miculescu, A.-C. Mocanu, A.E. Constantinescu, T.M. Butte, A.M. Pandele, R.-C. Ciocoiu, S.L. Voicu, L.T. Ciocan, Novel synthesis of core-shell biomaterials from polymeric filaments with a bioceramic coating for biomedical applications, Coatings 10 (2020), doi:10.3390/coatings10030283.

[79] C.E. Corcione, F. Scalera, F. Gervaso, F. Montagna, A. Sannino, A. Maffezzoli, One-step solvent-free process for the fabrication of high loaded PLA/HA composite filament for 3D printing, J. Therm. Anal. Calorim. 134 (2018) 575–582, doi:10.1007/s10973-018-7155-5.

[80] M. Bayart, M. Dubus, S. Charlon, H. Kerdjoudj, N. Baleine, S. Benali, J.-M. Raquez, J. Soulestin, Pellet-Based Fused Filament Fabrication (FFF)-derived process for the development of polylactic acid/hydroxyapatite scaffolds dedicated to bone regeneration, Materials 15 (2022), doi:10.3390/ma15165615.

[81] I. Fernandez-Cervantes, M.A. Morales, R. Agustin-Serrano, M. Cardenas-Garcia, P.V. Perez-Luna, B.L. Arroyo-Reyes, A. Maldonado-Garcia, Polylactic acid/sodium alginate/hydroxyapatite composite scaffolds with trabecular tissue morphology designed by a bone remodeling model using 3D printing, J. Mater. Sci. 54 (2019) 9478–9496, doi:10.1007/s10853-019-03537-1.

[82] T. Distler, N. Fournier, A. Gruenewald, C. Polley, H. Seitz, R. Detsch, A.R. Boccaccini, Polymer-bioactive glass composite filaments for 3D scaffold manufacturing by fused deposition modeling: fabrication and characterization, Front. Bioeng. Biotechnol. 8 (2020), doi:10.3389/fbioe.2020.00552.

[83] N.W. Pensa, A.S. Curry, P.P. Bonvallet, N.F. Bellis, K.M. Rettig, M.S. Reddy, A.W. Eberhardt, S.L. Bellis, 3D printed mesh reinforcements enhance the mechanical properties of electrospun scaffolds, Biomater. Res. 23 (2019), doi:10.1186/s40824-019-0171-0.

[84] H. Chen, H. Zhang, Y. Shen, X. Dai, X. Wang, K. Deng, X. Long, L. Liu, X. Zhang, Y. Li, T. Xu, Instant in-situ tissue repair by biodegradable PLA/gelatin nanofibrous membrane using a 3d printed handheld electrospinning device, Front. Bioeng. Biotechnol. 9 (2021) 684105, doi:10.3389/fbioe.2021.684105.

[85] V. Guduric, C. Metz, R. Siadous, R. Bareille, R. Levato, E. Engel, J.-C. Fricain, R. Devillard, O. Luzanin, S. Catros, Layer-by-layer bioassembly of cellularized polylactic acid porous membranes for bone tissue engineering, J. Mater. Sci. Mater. Med. 28 (2017) 78, doi:10.1007/s10856-017-5887-6.

[86] X. Liang, J. Gao, W. Xu, X. Wang, Y. Shen, J. Tang, S. Cui, X. Yang, Q. Liu, L. Yu, J. Ding, Structural mechanics of 3D-printed poly(lactic acid) scaffolds with tetragonal, hexagonal and wheel-like designs, Biofabrication 11 (2019), doi:10.1088/1758-5090/ab0f59.

[87] F. Azadmanesh, M. Pourmadadi, J. Zavar Reza, F. Yazdian, F. Omidi, B.F. Haghirosadat, Synthesis of a novel nanocomposite containing chitosan as a three-dimensional printed wound dressing technique: emphasis on gene expression, Biotechnol. Prog. 37 (2021) e3132, doi:10.1002/btpr.3132.

[88] J.A. Driscoll, R. Lubbe, A.E. Jakus, K. Chang, M. Haleem, C. Yun, G. Singh, A.D. Schneider, K.M. Katchko, C. Soriano, M. Newton, T. Maerz, X. Li, K. Baker, W.K. Hsu, R.N. Shah, S.R. Stock, E.L. Hsu, 3D-printed ceramic-demineralized

bone matrix hyperelastic bone composite scaffolds for spinal fusion, Tissue Eng. Part A 26 (2020) 157–166, doi:10.1089/ten.TEA.2019.0166.

[89] D. Gao, Z. Wang, Z. Wu, M. Guo, Y. Wang, Z. Gao, P. Zhang, Y. Ito, 3D-printing of solvent exchange deposition modeling (SEDM) for a bilayered flexible skin substitute of poly (lactide-co-glycolide) with bioorthogonally engineered EGF, Mater. Sci. Eng. C 112 (2020) 110942, doi:10.1016/j.msec.2020.110942.

[90] R. Fairag, L. Li, J.L. Ramirez-GarciaLuna, M.S. Taylor, B. Gaerke, M.H. Weber, D.H. Rosenzweig, L. Haglund, A composite lactide-mineral 3D-printed scaffold for bone repair and regeneration, Front. Cell Dev. Biol. 9 (2021), doi:10.3389/fcell.2021.654518.

[91] Y. Dou, J. Huang, X. Xia, J. Wei, Q. Zou, Y. Zuo, J. Li, Y. Li, A hierarchical scaffold with a highly pore-interconnective 3D printed PLGA/n-HA framework and an extracellular matrix like gelatin network filler for bone regeneration, J. Mater. Chem. B. 9 (2021) 4488–4501, doi:10.1039/d1tb00662b.

[92] H. Kang, X. Jiang, Z. Liu, F. Liu, G. Yan, F. Li, Biodegradable 3D printed scaffolds of modified poly (trimethylene lactide) composite materials with Poly (L-lactic acid) and hydroxyapatite for bone regeneration, Nanomaterials 11 (2021), doi:10.3390/nano11123215.

[93] S. Kurt, S. Selviler-Sizer, B. Onuk, M. Kabak, Comparison of sheep scapula models created with polylactic acid and thermoplastic polyurethane filaments by three-dimensional modelling, Anat. Histol. Embryol. 51 (2022) 244–249, doi:10.1111/ahe.12784.

[94] M. Micic, D. Antonijevic, S. Milutinovic-Smiljanic, D. Trisic, B. Colovic, D. Kosanovic, B. Prokic, J. Vasic, S. Zivkovic, J. Milasin, V. Danilovic, M. Djuric, V. Jokanovic, Developing a novel resorptive hydroxyapatite-based bone substitute for over-critical size defect reconstruction: physicochemical and biological characterization and proof of concept in segmental rabbit's ulna reconstruction, Biomed. Tech. 65 (2020) 491–505, doi:10.1515/bmt-2019-0218.

[95] J.W. Yun, S.Y. Heo, M.H. Lee, H.B. Lee, Evaluation of a poly(lactic-acid) scaffold filled with poly(lactide-co-glycolide)/hydroxyapatite nanofibres for reconstruction of a segmental bone defect in a canine model, Vet. Med. 64 (2019) 531–538, doi:10.17221/80/2019-VETMED.

[96] B. Zhang, S. Shen, H. Xian, Y. Dai, W. Guo, X. Li, X. Zhang, Z. Wang, H. Li, L. Peng, X. Luo, S. Liu, X. Lu, Q. Guo, Fabrication of poly (lactic-co-glycolic acid)/decellularized articular cartilage extracellular matrix scaffold by three-dimensional printing technology and investigating its physicochemical properties, J. Reparative Reconstr. Surg. 33 (2019) 1011–1018, doi:10.7507/1002-1892.201901082.

[97] B. Li, C. Ruan, Y. Ma, Z. Huang, Z. Huang, G. Zhou, J. Zhang, H. Wang, Z. Wu, G. Qiu, Fabrication of vascularized bone flaps with sustained release of recombinant human bone morphogenetic protein-2 and arteriovenous bundle, Tissue Eng. Part A. 24 (2018) 1413–1422, doi:10.1089/ten.TEA.2018.0002.

[98] S. Pitjamit, W. Nakkiew, K. Thongkorn, W. Thanakulwattana, K. Thunsiri, Finite element analysis of traditional and new fixation techniques of the 3D-printed composite interlocking nail in canine femoral shaft fractures, Appl. Sci.-BASEL. 10 (2020) 3424, doi:10.3390/app10103424.

[99] S. Camarero-Espinosa, L. Moroni, Janus 3D printed dynamic scaffolds for nanovibration-driven bone regeneration, Nat. Commun. 12 (2021) 1031, doi:10.1038/s41467-021-21325-x.

[100] M. Deng, J. Tan, C. Hu, T. Hou, W. Peng, J. Liu, B. Yu, Q. Dai, J. Zhou, Y. Yang, R. Dong, C. Ruan, S. Dong, J. Xu, Modification of PLGA scaffold by MSC-derived extracellular matrix combats macrophage inflammation to initiate bone regeneration via TGF-β-induced protein, Adv. Healthc. Mater. 9 (2020) e2000353, doi:10.1002/adhm.202000353.

[101] Y. Lai, Y. Li, H. Cao, J. Long, X. Wang, L. Li, C. Li, Q. Jia, B. Teng, T. Tang, J. Peng, D. Eglin, M. Alini, D.W. Grijpma, G. Richards, L. Qin, Osteogenic magnesium incorporated into PLGA/TCP porous scaffold by 3D printing for repairing challenging bone defect, Biomaterials 197 (2019) 207–219, doi:10.1016/j.biomaterials.2019.01.013.

[102] W.-X. Cheng, Y.-Z. Liu, X.-B. Meng, Z.-T. Zheng, L.-L. Li, L.-Q. Ke, L. Li, C.-S. Huang, G.-Y. Zhu, H.-D. Pan, L. Qin, X.-L. Wang, P. Zhang, PLGA/β-TCP composite scaffold incorporating cucurbitacin B promotes bone regeneration by inducing angiogenesis, J. Orthop. Transl. 31 (2021) 41–51, doi:10.1016/j.jot.2021.10.002.

[103] W. Yu, R. Li, J. Long, P. Chen, A. Hou, L. Li, X. Sun, G. Zheng, H. Meng, Y. Wang, A. Wang, X. Sui, Q. Guo, S. Tao, J. Peng, L. Qin, S. Lu, Y. Lai, Use of a three-dimensional printed polylactide-coglycolide/tricalcium phosphate composite scaffold incorporating magnesium powder to enhance bone defect repair in rabbits, J. Orthop. Transl. 16 (2019) 62–70, doi:10.1016/j.jot.2018.07.007.

[104] J. Wei, Y. Yan, J. Gao, Y. Li, R. Wang, J. Wang, Q. Zou, Y. Zuo, M. Zhu, J. Li, 3D-printed hydroxyapatite microspheres reinforced PLGA scaffolds for bone regeneration, Mater. Sci. Eng. C (2021) 112618, doi:10.1016/j.msec.2021.112618.

[105] W. Chen, L. Nichols, L. Teer, K. Clinton, L.B. Priddy, A hybrid coating of polydopamine and nano-hydroxyapatite enhances surface properties of 3D printed poly(lactic-co-glycolic acid) scaffolds, J. Mater. Sci. 57 (2022) 13011–13026, doi:10.1007/s10853-022-07442-y.

[106] M. Lian, Y. Han, B. Sun, L. Xu, X. Wang, B. Ni, W. Jiang, Z. Qiao, K. Dai, X. Zhang, A multifunctional electrowritten bi-layered scaffold for guided bone regeneration, Acta Biomater. 118 (2020) 83–99, doi:10.1016/j.actbio.2020.08.017.

[107] C. Shuai, W. Yang, P. Feng, S. Peng, H. Pan, Accelerated degradation of HAP/PLLA bone scaffold by PGA blending facilitates bioactivity and osteoconductivity, Bioact. Mater. 6 (2021) 490–502, doi:10.1016/j.bioactmat.2020.09.001.

[108] R. Donate, M. Monzon, M.E. Aleman-Dominguez, Additive manufacturing of PLA-based scaffolds intended for bone regeneration and strategies to im-

[109] prove their biological properties, E-Polym. 20 (2020) 571–599, doi:10.1515/epoly-2020-0046.

[109] J. Babilotte, B. Martin, V. Guduric, R. Bareille, R. Agniel, S. Roques, V. Héroguez, M. Dussauze, M. Gaudon, D. Le Nihouannen, S. Catros, Development and characterization of a PLGA-HA composite material to fabricate 3D-printed scaffolds for bone tissue engineering, Mater. Sci. Eng. C 118 (2021) 111334, doi:10.1016/j.msec.2020.111334.

[110] Z. Xu, N. Wang, P. Liu, Y. Sun, Y. Wang, F. Fei, S. Zhang, J. Zheng, B. Han, Poly(Dopamine) coating on 3D-printed poly-lactic-co-glycolic acid/β-tricalcium phosphate scaffolds for bone tissue engineering, Molecules 24 (2019), doi:10.3390/molecules24234397.

[111] P.-C. Chang, H.-T. Luo, Z.-J. Lin, W.-C. Tai, C.-H. Chang, Y.-C. Chang, D.L. Cochran, M.-H. Chen, Preclinical evaluation of a 3D-printed hydroxyapatite/poly(lactic-co-glycolic acid) scaffold for ridge augmentation, J. Formos. Med. Assoc. Taiwan Yi Zhi. 120 (2021) 1100–1107, doi:10.1016/j.jfma.2020.10.022.

[112] S.-S. Cao, S.-Y. Li, Y.-M. Geng, K. Kapat, S.-B. Liu, F.H. Perera, Q. Li, H. Terheyden, G. Wu, Y.-J. Che, P. Miranda, M. Zhou, Prefabricated 3D-printed tissue-engineered bone for mandibular reconstruction: a preclinical translational study in primate, ACS Biomater. Sci. Eng. 7 (2021) 5727–5738, doi:10.1021/acsbiomaterials.1c00509.

[113] P.-C. Chang, H.-T. Luo, Z.-J. Lin, W.-C. Tai, C.-H. Chang, Y.-C. Chang, D.L. Cochran, M.-H. Chen, Regeneration of critical-sized mandibular defect using a 3D-printed hydroxyapatite-based scaffold: an exploratory study, J. Periodontol. 92 (2021) 428–435, doi:10.1002/JPER.20-0110.

[114] S.K. Lee, C.-M. Han, W. Park, I.H. Kim, Y.K. Joung, D.K. Han, Synergistically enhanced osteoconductivity and anti-inflammation of PLGA/β-TCP/Mg(OH)(2) composite for orthopedic applications, Mater. Sci. Eng. C 94 (2019) 65–75, doi:10.1016/j.msec.2018.09.011.

[115] H. Liu, H. Zhu, L. Cheng, Y. Zhao, X. Chen, J. Li, X. Xv, Z. Xiao, W. Li, J. Pan, Q. Zhang, C. Zeng, J. Guo, D. Xie, D. Cai, TCP/PLGA composite scaffold loaded rapamycin in situ enhances lumbar fusion by regulating osteoblast and osteoclast activity, J. Tissue Eng. Regen. Med. 15 (2021) 475–486, doi:10.1002/term.3186.

[116] R. Duan, Y. Wang, D. Su, Z. Wang, Y. Zhang, B. Du, L. Liu, X. Li, Q. Zhang, The effect of blending poly (l-lactic acid) on in vivo performance of 3D-printed poly(l-lactide-co-caprolactone)/PLLA scaffolds, Biomater. Adv. 138 (2022) 212948, doi:10.1016/j.bioadv.2022.212948.

[117] E. Akerlund, A. Diez-Escudero, A. Grzeszczak, C. Persson, The effect of PCL addition on 3D-printable PLA/HA composite filaments for the treatment of bone defects, Polymers 14 (2022), doi:10.3390/polym14163305.

[118] S. Pitjamit, K. Thunsiri, W. Nakkiew, T. Wongwichai, P. Pothacharoen, W. Wattanutchariya, The possibility of interlocking nail fabrication from FFF 3D printing PLA/PCL/HA composites coated by local silk fibroin for canine bone fracture treatment, Materials 13 (2020), doi:10.3390/ma13071564.

[119] J. Pizzicannella, F. Diomede, A. Gugliandolo, L. Chiricosta, P. Bramanti, I. Merciaro, T. Orsini, E. Mazzon, O. Trubiani, 3D Printing PLA/gingival stem cells/EVs upregulate miR-2861 and -210 during osteoangiogenesis commitment, Int. J. Mol. Sci. 20 (2019), doi:10.3390/ijms20133256.

[120] Z.B. Velioglu, D. Pulat, B. Demirbakan, B. Ozcan, E. Bayrak, C. Erisken, 3D-printed poly(lactic acid) scaffolds for trabecular bone repair and regeneration: scaffold and native bone characterization, Connect. Tissue Res. 60 (2019) 274–282, doi:10.1080/03008207.2018.1499732.

[121] N. Söhling, J. Neijhoft, V. Nienhaus, V. Acker, J. Harbig, F. Menz, J. Ochs, R.D.R.D. Verboket, U. Ritz, A. Blaeser, E. Dörsam, J. Frank, I. Marzi, D. Henrich, N. Soehling, J. Neijhoft, V. Nienhaus, V. Acker, J. Harbig, F. Menz, J. Ochs, R.D.R.D. Verboket, U. Ritz, A. Blaeser, E. Doersam, J. Frank, I. Marzi, D. Henrich, N. Söhling, J. Neijhoft, V. Nienhaus, V. Acker, J. Harbig, F. Menz, J. Ochs, R.D.R.D. Verboket, U. Ritz, A. Blaeser, E. Dörsam, J. Frank, I. Marzi, D. Henrich, 3D-Printing of hierarchically designed and osteoconductive bone tissue engineering scaffolds, MATERIALS. 13 (2020), doi:10.3390/ma13081836.

[122] A. Lauer, P. Wolf, D. Mehler, H. Goetz, M. Ruezgar, A. Baranowski, D. Henrich, P.M. Rommens, U. Ritz, Biofabrication of SDF-1 functionalized 3D-printed cell-free scaffolds for bone tissue regeneration, Int. J. Mol. Sci. 21 (2020), doi:10.3390/ijms21062175.

[123] S.H. Han, M. Cha, Y.-Z. Jin, K.-M. Lee, J.H. Lee, BMP-2 and hMSC dual delivery onto 3D printed PLA-Biogel scaffold for critical-size bone defect regeneration in rabbit tibia, Biomed. Mater. 16 (2021) 15019, doi:10.1088/1748-605X/aba879.

[124] C.-H. Yao, Y.-H. Lai, Y.-W. Chen, C.-H. Cheng, Bone morphogenetic protein-2-activated 3D-printed polylactic acid scaffolds to promote bone regrowth and repair, Macromol. Biosci. 20 (2020) e2000161, doi:10.1002/mabi.202000161.

[125] R.T. Anbu, V. Suresh, R. Gounder, A. Kannan, Comparison of the efficacy of three different bone regeneration materials: an animal study, Eur. J. Dent. 13 (2019) 22–28, doi:10.1055/s-0039-1688735.

[126] M. Zhu, J. Tan, L. Liu, J. Tian, L. Li, B. Luo, C. Zhou, L. Lu, Construction of biomimetic artificial intervertebral disc scaffold via 3D printing and electrospinning, Mater. Sci. Eng. C 128 (2021), doi:10.1016/j.msec.2021.112310.

[127] M. Alksne, M. Kalvaityte, E. Simoliunas, I. Gendviliene, P. Barasa, I. Rinkunaite, A. Kaupinis, D. Seinin, V. Rutkunas, V. Bukelskiene, Dental pulp stem cell-derived extracellular matrix: autologous tool boosting bone regeneration, Cytotherapy 24 (2022) 597–607, doi:10.1016/j.jcyt.2022.02.002.

[128] B.N. Teixeira, P. Aprile, R.H. Mendonça, D.J. Kelly, R.M.D.S.M. Thiré, Evaluation of bone marrow stem cell response to PLA scaffolds manufactured by 3D printing and coated with polydopamine and type I collagen, J. Biomed. Mater. Res. Part B 107 (2019) 37–49, doi:10.1002/jbm.b.34093.

[129] X. Zhang, Q. Lou, L. Wang, S. Min, M. Zhao, C. Quan, Immobilization of BMP-2-derived peptides on 3D-printed porous scaffolds for enhanced osteogenesis, Biomed. Mater. Bristol Engl. 15 (2019) 15002, doi:10.1088/1748-605X/ab4c78.

[130] L. Perez-Sanchez, M.A.O. De la O, P. Gonzalez-Alva, L.A. Medina, D. Masuoka-Ito, M.A. Alvarez-Perez, J. Serrano-Bello, In vivo study on bone response to 3D-printed constructs designed from microtomographic images, J. Mater. Eng. Perform. 30 (2021) 5005–5012, doi:10.1007/s11665-021-05585-8.

[131] A. Sharma, S. Gupta, T.S. Sampathkumar, R.S. Verma, Modified graphene oxide nanoplates reinforced 3D printed multifunctional scaffold for bone tissue engineering, Biomater. Adv. 134 (2022) 112587, doi:10.1016/j.msec.2021.112587.

[132] K.-S. Liu, W.-H. Chen, C.-H. Lee, Y.-F. Su, Y.-W. Liu, S.-J. Liu, Novel biodegradable 3D-printed analgesics-eluting-nanofibers incorporated nuss bars for therapy of pectus excavatum, Int. J. Mol. Sci. 23 (2022) 2265, doi:10.3390/ijms23042265.

[133] J.L. Chakka, T. Acri, N.Z. Laird, L. Zhong, K. Shin, S. Elangovan, A.K. Salem, Polydopamine functionalized VEGF gene-activated 3D printed scaffolds for bone regeneration, RSC Adv. 11 (2021) 13282–13291, doi:10.1039/d1ra01193f.

[134] P. Wang, H.-M. Yin, X. Li, W. Liu, Y.-X. Chu, Y. Wang, Y. Wang, J.-Z. Xu, Z.-M. Li, J.-H. Li, Simultaneously constructing nanotopographical and chemical cues in 3D-printed polylactic acid scaffolds to promote bone regeneration, Mater. Sci. Eng. C 118 (2021), doi:10.1016/j.msec.2020.111457.

[135] J. Yun, J. Lee, C.W. Ha, S.J. Park, S. Kim, K. Koo, Y. Seol, Y. Lee, The effect of 3-D printed polylactic acid scaffold with and without hyaluronic acid on bone regeneration, J. Periodontol. (2022) 1–11, doi:10.1002/jper.21-0428.

[136] M. Bahraminasab, A. Talebi, N. Doostmohammadi, S. Arab, A. Ghanbari, S. Zarbakhsh, The healing of bone defects by cell-free and stem cell-seeded 3D-printed PLA tissue-engineered scaffolds, J. Orthop. Surg. 17 (2022) 320, doi:10.1186/s13018-022-03213-2.

[137] F. Diomede, A. Gugliandolo, P. Cardelli, I. Merciaro, V. Ettorre, T. Traini, R. Bedini, D. Scionti, A. Bramanti, A. Nanci, S. Caputi, A. Fontana, E. Mazzon, O. Trubiani, Three-dimensional printed PLA scaffold and human gingival stem cell-derived extracellular vesicles: a new tool for bone defect repair, Stem Cell Res. Ther. 9 (2018), doi:10.1186/s13287-018-0850-0.

[138] M. Cha, Y.-Z. Jin, J.W. Park, K.M. Lee, S.H. Han, B.S. Choi, J.H. Lee, Three-dimensional printed polylactic acid scaffold integrated with BMP-2 laden hydrogel for precise bone regeneration, Biomater. Res. 25 (2021), doi:10.1186/s40824-021-00233-7.

[139] H. Chen, Q. Shi, H. Shui, P. Wang, Q. Chen, Z. Li, Degradation of 3D-printed porous polylactic acid scaffolds under mechanical stimulus, Front. Bioeng. Biotechnol. 9 (2021), doi:10.3389/fbioe.2021.691834.

[140] P. Karimipour-Fard, R. Pop-Iliev, H. Jones-Taggart, G. Rizvi, G.U. Erinc, Design of 3D scaffold geometries for optimal biodegradation of poly(lactic acid)-based bone tissue, in: Proc. 35TH Int. Conf. Polym. Process. Soc. PPS-35, 2020, p. 2205, doi:10.1063/1.5142977.

[141] H. Shui, Q. Shi, N.M. Pugno, Q. Chen, Z. Li, Effect of mechanical stimulation on the degradation of poly(lactic acid) scaffolds with different designed structures, J. Mech. Behav. Biomed. Mater. 96 (2019) 324–333, doi:10.1016/j.jmbbm.2019.04.028.

[142] S.C. Cifuentes, L. Saldana, J.Luis Gonzalez-Carrasco, R. Benavente, A. Garcia-Penas, Effect of thermal processing on the dynamic/isothermal crystallization and cytocompatibility of polylactic acid for biomedical applications, Macromol. Chem. Phys. 222 (2021), doi:10.1002/macp.202100274.

[143] E. Mohan, M.S. Kumar, Experimental investigation on mechanical and tribological properties of the fused filament fabrication of poly-lactic acid parts with various print orientations, Appl. Phys. 128 (2022), doi:10.1007/s00339-022-05579-w.

[144] Y. Zhang, C. Wang, L. Fu, S. Ye, M. Wang, Y. Zhou, Fabrication and application of novel bioactive scaffold in situ-loaded graphene oxide and osteogenic peptide by cryogenic 3D printing for repairing critical-sized bone defect, Molecules 24 (2019), doi:10.3390/molecules24091669.

[145] A.C.D. Nascimento Jr., R.C.D.A.G. Mota, L.R.D. Menezes, E.O.D. Silva, Influence of the printing parameters on the properties of Poly(lactic acid) scaffolds obtained by fused deposition modeling 3D printing, Polym. Polym. Compos. 29 (2021) S1052–S1062, doi:10.1177/09673911211040770.

[146] B. Gao, H. Jing, M. Gao, S. Wang, W. Fu, X. Zhang, X. He, J. Zheng, Long-segmental tracheal reconstruction in rabbits with pedicled Tissue-engineered trachea based on a 3D-printed scaffold, Acta Biomater. 97 (2019) 177–186, doi:10.1016/j.actbio.2019.07.043.

[147] C. Pagano, L. Rebaioli, F. Baldi, I. Fassi, G.U. Erinc, Mechanical behavior of scaffold-like structures: research of relationships between properties and geometry, in: Proc. 35TH Int. Conf. Polym. Process. Soc. PPS-35, 2020, p. 2205, doi:10.1063/1.5142979.

[148] R. Baptista, M. Guedes, Morphological and mechanical characterization of 3D printed PLA scaffolds with controlled porosity for trabecular bone tissue replacement, Mater. Sci. Eng. C 118 (2021), doi:10.1016/j.msec.2020.111528.

[149] R. Baptista, M. Guedes, Porosity and pore design influence on fatigue behavior of 3D printed scaffolds for trabecular bone replacement, J. Mech. Behav. Biomed. Mater. 117 (2021), doi:10.1016/j.jmbbm.2021.104378.

[150] D. Singh, A. Babbar, V. Jain, D. Gupta, S. Saxena, V. Dwibedi, Synthesis, characterization, and bioactivity investigation of biomimetic biodegradable PLA scaffold fabricated by fused filament fabrication process, J. Braz. Soc. Mech. Sci. Eng. 41 (2019), doi:10.1007/s40430-019-1625-y.

[151] K.-C. Feng, A. Pinkas-Sarafova, V. Ricotta, M. Cuiffo, L. Zhang, Y. Guo, C.-C. Chang, G.P. Halada, M. Simon, M. Rafailovich, The influence of roughness on stem cell differentiation using 3D printed polylactic acid scaffolds, Soft Matter 14 (2018) 9838–9846, doi:10.1039/c8sm01797b.

[152] A. Grivet-Brancot, M. Boffito, G. Ciardelli, Use of polyesters in fused deposition modeling for biomedical applications, Macromol. Biosci. 22 (2022), doi:10.1002/mabi.202200039.

[153] Y.K. Yeon, H.S. Park, J.M. Lee, J.S. Lee, Y.J. Lee, Md.T. Sultan, Y.B. Seo, O.J. Lee, S.H. Kim, C.H. Park, New concept of 3D printed bone clip (polylactic acid/hydroxyapatite/silk composite) for internal fixation of bone fractures, J. Biomater. Sci. 29 (2018) 894–906, doi:10.1080/09205063.2017.1384199.

[154] X. Chen, C. Gao, J. Jiang, Y. Wu, P. Zhu, G. Chen, 3D printed porous PLA/nHA composite scaffolds with enhanced osteogenesis and osteoconductivity in vivo for bone regeneration, Biomed. Mater. 14 (2019), doi:10.1088/1748-605X/ab388d.

[155] Z. Liu, Y. Ge, L. Zhang, Y. Wang, C. Guo, K. Feng, S. Yang, Z. Zhai, Y. Chi, J. Zhao, F. Liu, The effect of induced membranes combined with enhanced bone marrow and 3D PLA-HA on repairing long bone defects in vivo, J. TISSUE Eng. Regen. Med. 14 (2020) 1403–1414, doi:10.1002/term.3106.

[156] W. Wang, B. Zhang, M. Li, J. Li, C. Zhang, Y. Han, L. Wang, K. Wang, C. Zhou, L. Liu, Y. Fan, X. Zhang, 3D printing of PLA/n-HA composite scaffolds with customized mechanical properties and biological functions for bone tissue engineering, Compos. Part B 224 (2021) 109192, doi:10.1016/j.compositesb.2021.109192.

[157] W. Wang, B. Zhang, L. Zhao, M. Li, Y. Han, L. Wang, Z. Zhang, J. Li, C. Zhou, L. Liu, Fabrication and properties of PLA/nano-HA composite scaffolds with balanced mechanical properties and biological functions for bone tissue engineering application, Nanotechnol. Rev. 10 (2021) 1359–1373, doi:10.1515/ntrev-2021-0083.

[158] B. Zhang, L. Wang, P. Song, X. Pei, H. Sun, L. Wu, C. Zhou, K. Wang, Y. Fan, X. Zhang, 3D printed bone tissue regenerative PLA/HA scaffolds with comprehensive performance optimizations, Mater. Des. 201 (2021) 109490, doi:10.1016/j.matdes.2021.109490.

[159] H. Zhang, X. Mao, D. Zhao, W. Jiang, Z. Du, Q. Li, C. Jiang, D. Han, Three dimensional printed polylactic acid-hydroxyapatite composite scaffolds for prefabricating vascularized tissue engineered bone: an in vivo bioreactor model, Sci. Rep. 7 (2017) 15255, doi:10.1038/s41598-017-14923-7.

[160] B.W. Minto, A.G. Sprada, J.A. Gonçalves Neto, B.M. de Alcântara, T.A.S. de S. Rocha, A.C.V. Hespanha, C. Quarterone, M. da R. Sartori, A. Hataka, R.A.R. Uscategui, L.G.G.G. Dias, Three-dimensional printed poly (L-lactide) and hydroxyapatite composite for reconstruction of critical bone defect in rabbits, Acta Cirúrgica Bras 36 (2021) e360404, doi:10.1590/acb360404.

[161] I. Gendviliene, E. Simoliunas, M. Alksne, S. Dibart, E. Jasiuniene, V. Cicenas, R. Jacobs, V. Bukelskiene, V. Rutkunas, Effect of extracellular matrix and dental pulp stem cells on bone regeneration with 3D printed PLA/HA composite scaffolds, Eur. Cell Mater. 41 (2021) 204–215, doi:10.22203/eCM.v041a15.

[162] M.O.C. Maia-Pinto, A.C.B. Brochado, B.N. Teixeira, S.C. Sartoretto, M.J. Uzeda, A.T.N.N. Alves, G.G. Alves, M.D. Calasans-Maia, R.M.S.M. Thiré, Biomimetic mineralization on 3D printed PLA scaffolds: on the response of human primary osteoblasts spheroids and in vivo implantation, Polymers 13 (2020) 74, doi:10.3390/polym13010074.

[163] C. Tu, J. Chen, C. Huang, Y. Xiao, X. Tang, H. Li, Y. Ma, J. Yan, W. Li, H. Wu, C. Liu, Effects of electromagnetic fields treatment on rat critical-sized calvarial defects with a 3D-printed composite scaffold, Stem Cell Res. Ther. 11 (2020) 433, doi:10.1186/s13287-020-01954-7.

[164] D.Y. Kwon, J.H. Park, S.H. Jang, J.Y. Park, J.W. Jang, B.H. Min, W.-D. Kim, H.B. Lee, J. Lee, M.S. Kim, Bone regeneration by means of a three-dimensional printed scaffold in a rat cranial defect, J. Tissue Eng. Regen. Med. 12 (2018) 516–528, doi:10.1002/term.2532.

[165] I. Tcacencu, N. Rodrigues, N. Alharbi, M. Benning, S. Toumpaniari, E. Mancuso, M. Marshall, O. Bretcanu, M. Birch, A. McCaskie, K. Dalgarno, Osseointegration of porous apatite-wollastonite and poly(lactic acid) composite structures created using 3D printing techniques, Mater. Sci. Eng. C 90 (2018) 1–7, doi:10.1016/j.msec.2018.04.022.

[166] H. Zhang, X. Mao, Z. Du, W. Jiang, X. Han, D. Zhao, D. Han, Q. Li, Three dimensional printed macroporous polylactic acid/hydroxyapatite composite scaffolds for promoting bone formation in a critical-size rat calvarial defect model, Sci. Technol. Adv. Mater. 17 (2016) 136–148, doi:10.1080/14686996.2016.1145532.

[167] Z. Xu, B. Lin, C. Zhao, Y. Lu, T. Huang, Y. Chen, J. Li, R. Wu, W. Liu, J. Lin, Lanthanum doped octacalcium phosphate/polylactic acid scaffold fabricated by 3D printing for bone tissue engineering, J. Mater. Sci. Technol. 118 (2022) 229–242, doi:10.1016/j.jmst.2021.09.069.

[168] N.P. Tipnis, D.J. Burgess, Sterilization of implantable polymer-based medical devices: a review, Int. J. Pharm. 544 (2018) 455–460, doi:10.1016/j.ijpharm.2017.12.003.

[169] L.-C. Gerhardt, A.R. Boccaccini, Bioactive glass and glass-ceramic scaffolds for bone tissue engineering, Materials 3 (2010) 3867–3910, doi:10.3390/ma3073867.

[170] K. Hayashi, M.L. Munar, K. Ishikawa, Effects of macropore size in carbonate apatite honeycomb scaffolds on bone regeneration, Mater. Sci. Eng. C. 111 (2020) 110848, doi:10.1016/j.msec.2020.110848.

[171] A.R. Amini, C.T. Laurencin, S.P. Nukavarapu, Bone Tissue Engineering: Recent Advances and Challenges, 2013.

[172] N. Abbasi, S. Hamlet, R.M. Love, N.-T. Nguyen, Porous scaffolds for bone regeneration, J. Sci. Adv. Mater. Devices. 5 (2020) 1–9, doi:10.1016/j.jsamd.2020.01.007.

[173] S.G. Pedrero, P. Llamas-Sillero, J. Serrano-López, A multidisciplinary journey towards bone tissue engineering, Materials 14 (2021) 4896, doi:10.3390/ma14174896.

[174] K.-W. Chong, C.Y.-L. Woon, M.-K. Wong, Induced membranes—a staged technique of bone-grafting for segmental bone loss: surgical technique, J. Bone Jt. Surg. 93 (2011) 85–91, doi:10.2106/JBJS.J.01251.

[175] B. Zhang, L. Wang, P. Song, X. Pei, H. Sun, L. Wu, C. Zhou, K. Wang, Y. Fan, X. Zhang, 3D printed bone tissue regenerative PLA/HA scaffolds with comprehensive performance optimizations, Mater. Des. 201 (2021), doi:10.1016/j.matdes.2021.109490.

[176] R.-S. Chen, S.-H. Hsu, H.-H. Chang, M.-H. Chen, Challenge tooth regeneration in adult dogs with dental pulp stem cells on 3D-printed hydroxyapatite/polylactic acid scaffolds, CELLS 10 (2021), doi:10.3390/cells10123277.

[177] A.M. Maadani, E. Salahinejad, Performance comparison of PLA- and PLGA-coated porous bioceramic scaffolds: mechanical, biodegradability, bioactivity, delivery and biocompatibility assessments, J. Controlled Release 351 (2022) 1–7, doi:10.1016/j.jconrel.2022.09.022.

[178] Y. Zhao, B. Zhu, Y. Wang, C. Liu, C. Shen, Effect of different sterilization methods on the properties of commercial biodegradable polyesters for single-use, disposable medical devices, Mater. Sci. Eng. C 105 (2019) 110041, doi:10.1016/j.msec.2019.110041.

[179] N.S. Turker, A.Y. Özer, Ş. Çolak, B. Kutlu, R. Nohutçu, ESR investigations of gamma irradiated medical devices, Appl. Radiat. Isot. 130 (2017) 121–130, doi:10.1016/j.apradiso.2017.09.026.

[180] S. Pérez-Davila, L. González-Rodríguez, R. Lama, M. López-Álvarez, A.L. Oliveira, J. Serra, B. Novoa, A. Figueras, P. González, 3D-Printed PLA medical devices: physicochemical changes and biological response after sterilisation treatments, Polymers 14 (2022) 4117, doi:10.3390/polym14194117.

[181] S. Zeiter, K. Koschitzki, M. Alini, F. Jakob, M. Rudert, M. Herrmann, Evaluation of preclinical models for the testing of bone tissue-engineered constructs, Tissue Eng. Part C 26 (2020) 107–117, doi:10.1089/ten.tec.2019.0213.

[182] L. Carbone, J. Austin, Pain and laboratory animals: publication practices for better data reproducibility and better animal welfare, PLoS ONE 11 (2016) e0155001, doi:10.1371/journal.pone.0155001.

[183] M.K. Huss, S.A. Felt, C. Pacharinsak, Influence of pain and analgesia on orthopedic and wound-healing models in rats and mice, Comp. Med. 69 (2019) 535–545, doi:10.30802/AALAS-CM-19-000013.

[184] M. Guarnieri, C. Brayton, L. DeTolla, N. Forbes-McBean, R. Sarabia-Estrada, P. Zadnik, Safety and efficacy of buprenorphine for analgesia in laboratory mice and rats, Lab. Anim. 41 (2012) 337–343, doi:10.1038/laban.152.

[185] L. Benato, N.J. Rooney, J.C. Murrell, Pain and analgesia in pet rabbits within the veterinary environment: a review, Vet. Anaesth. Analg. 46 (2019) 151–162, doi:10.1016/j.vaa.2018.10.007.

[186] P. Leucht, J.-B. Kim, R. Wazen, J.A. Currey, A. Nanci, J.B. Brunski, J.A. Helms, Effect of mechanical stimuli on skeletal regeneration around implants, Bone 40 (2007) 919–930, doi:10.1016/j.bone.2006.10.027.

[187] N. Mangir, S. Dikici, F. Claeyssens, S. MacNeil, Using *ex Ovo* Chick Chorioallantoic Membrane (CAM) assay to evaluate the biocompatibility and angiogenic response to biomaterials, ACS Biomater. Sci. Eng. 5 (2019) 3190–3200, doi:10.1021/acsbiomaterials.9b00172.

[188] I. Moreno-Jiménez, J.M. Kanczler, G. Hulsart-Billstrom, S. Inglis, R.O.C. Oreffo, The chorioallantoic membrane assay for biomaterial testing in tissue engineering: an *in vivo* preclinical model, Tissue Eng. Part C 23 (2017) 938–952, doi:10.1089/ten.tec.2017.0186.

[189] P. Bédard, S. Gauvin, K. Ferland, C. Caneparo, È. Pellerin, S. Chabaud, S. Bolduc, Innovative human three-dimensional tissue-engineered models as an alternative to animal testing, Bioengineering 7 (2020) 115, doi:10.3390/bioengineering7030115.

[190] E. Petrovova, Preclinical alternative model for analysis of porous scaffold biocompatibility in bone tissue engineering, ALTEX 36 (2019) 121–130, doi:10.14573/altex.1807241.

[191] A. Weigand, J.P. Beier, A. Arkudas, M. Al-Abboodi, E. Polykandriotis, R.E. Horch, A.M. Boos, The Arteriovenous (AV) loop in a small animal model to study angiogenesis and vascularized tissue engineering, J. Vis. Exp. 54676 (2016), doi:10.3791/54676.

[192] M. Bouyer, C. Garot, P. Machillot, J. Vollaire, V. Fitzpatrick, S. Morand, J. Boutonnat, V. Josserand, G. Bettega, C. Picart, 3D-printed scaffold combined to 2D osteoinductive coatings to repair a critical-size mandibular bone defect, Mater. Today Bio 11 (2021) 100113, doi:10.1016/j.mtbio.2021.100113.

[193] W. Wang, J. Wei, D. Lei, S. Wang, B. Zhang, S. Shang, B. Bai, C. Zhao, W. Zhang, C. Zhou, H. Zhou, S. Feng, 3D printing of lithium osteogenic bioactive composite scaffold for enhanced bone regeneration, Compos. Part B 256 (2023) 110641, doi:10.1016/j.compositesb.2023.110641.